# Search for Higgs boson decay to a charm quark-antiquark pair in proton-proton collisions at $\sqrt{s}$ = 13 TeV at CMS

*Based on arXiv:2205.05550, CMS-PAS-HIG-21-008*

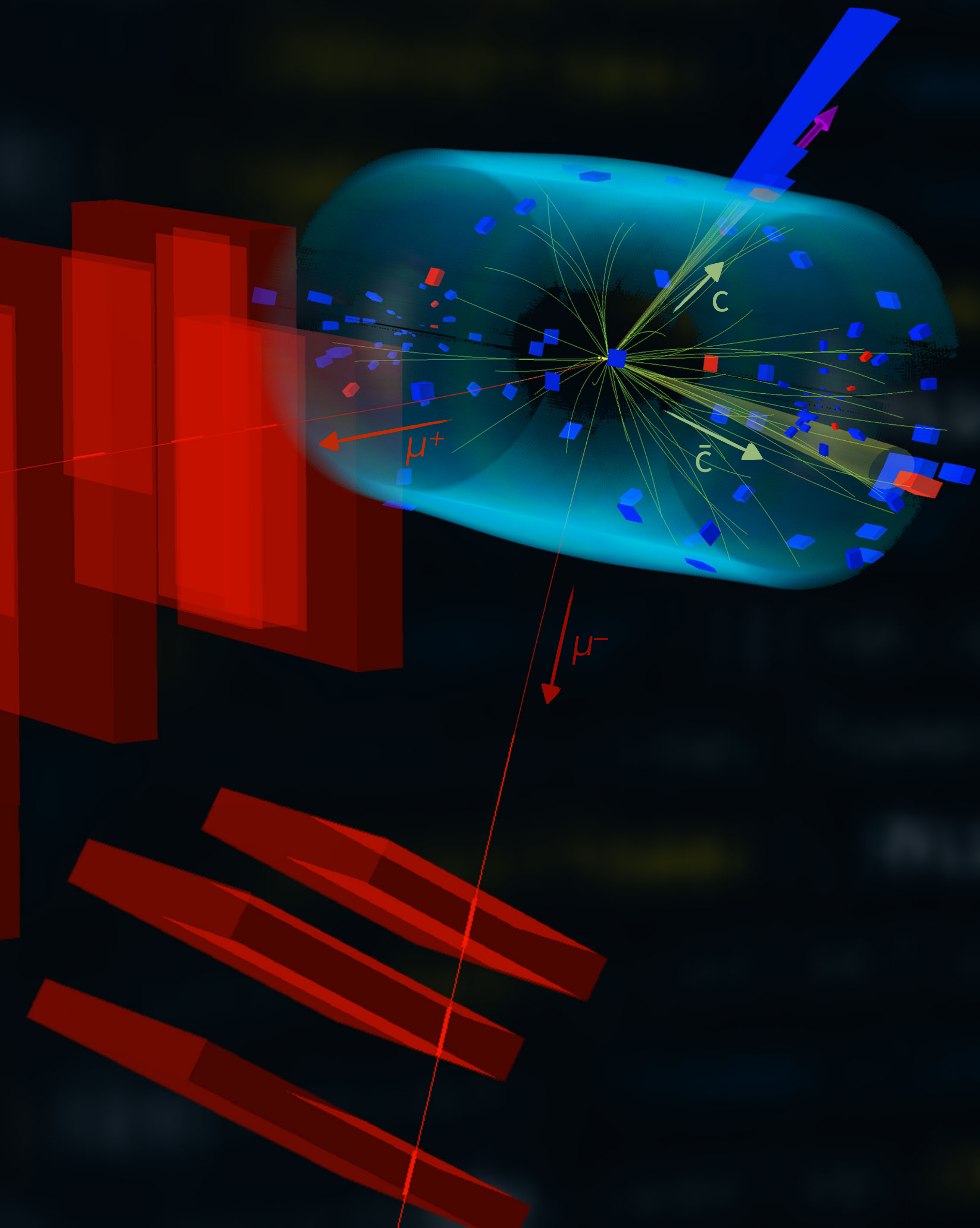


**Congqiao Li** (李聪乔), *Peking University*

中国物理学会高能物理分会第十一届全国会员代表大会
暨学术年会 · 大连

*10 Aug, 2022*

# Motivation

- Measurement of the Higgs boson properties is of vital importance since its discovery
  - couplings with 3rd generation fermions (t/b/τ) well-measured in high precision
- Next milestone: measure Yukawa couplings with 2nd generation fermions
  - **Higgs-charm** coupling can be modified in some BSM scenarios → essential to verify SM prediction and find possible hints to BSM
  - direct approach: **measure Higgs-charm coupling via H→cc decay channel**

*Higgs coupling measurement*

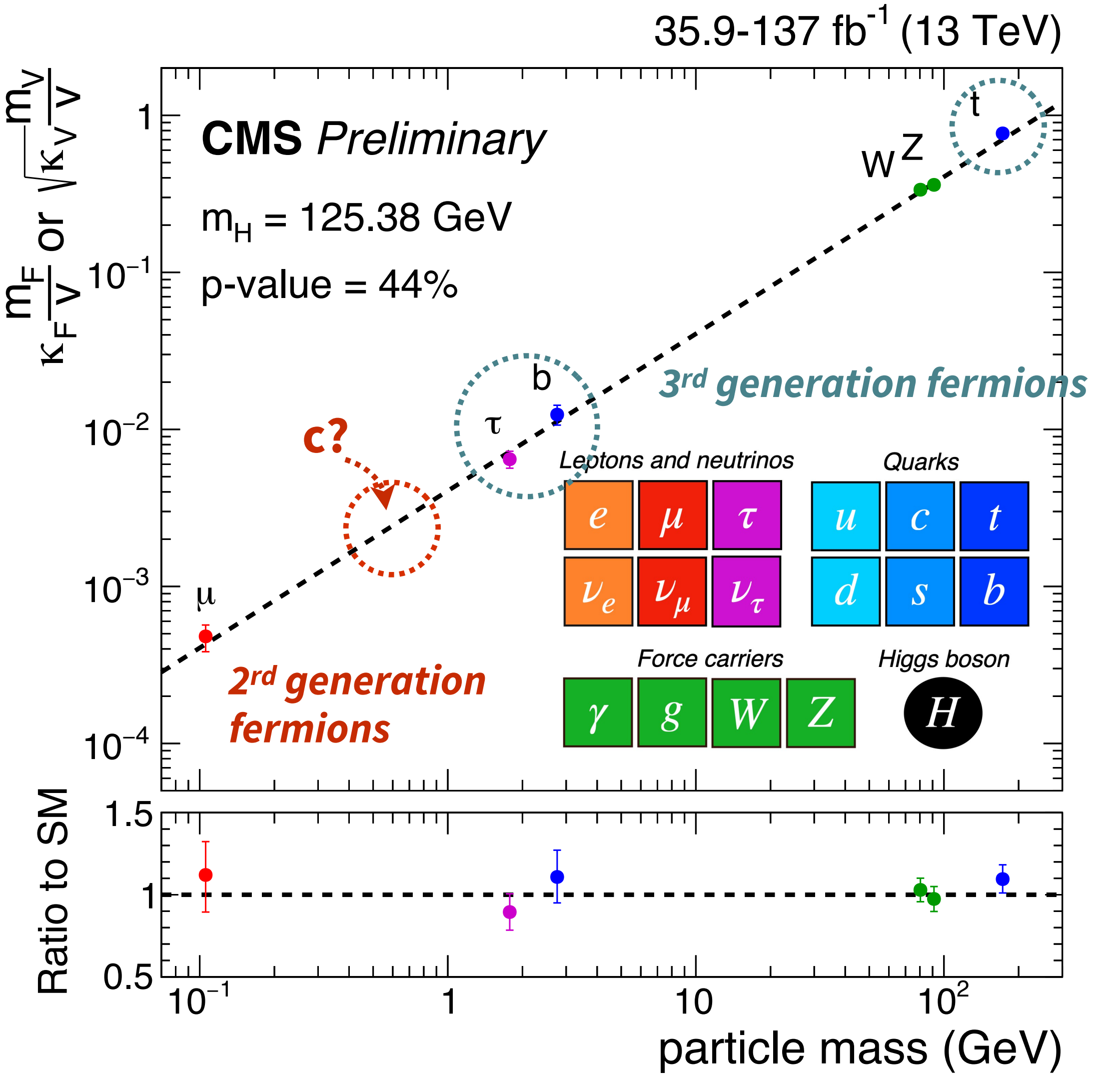

# Journey of VHcc search

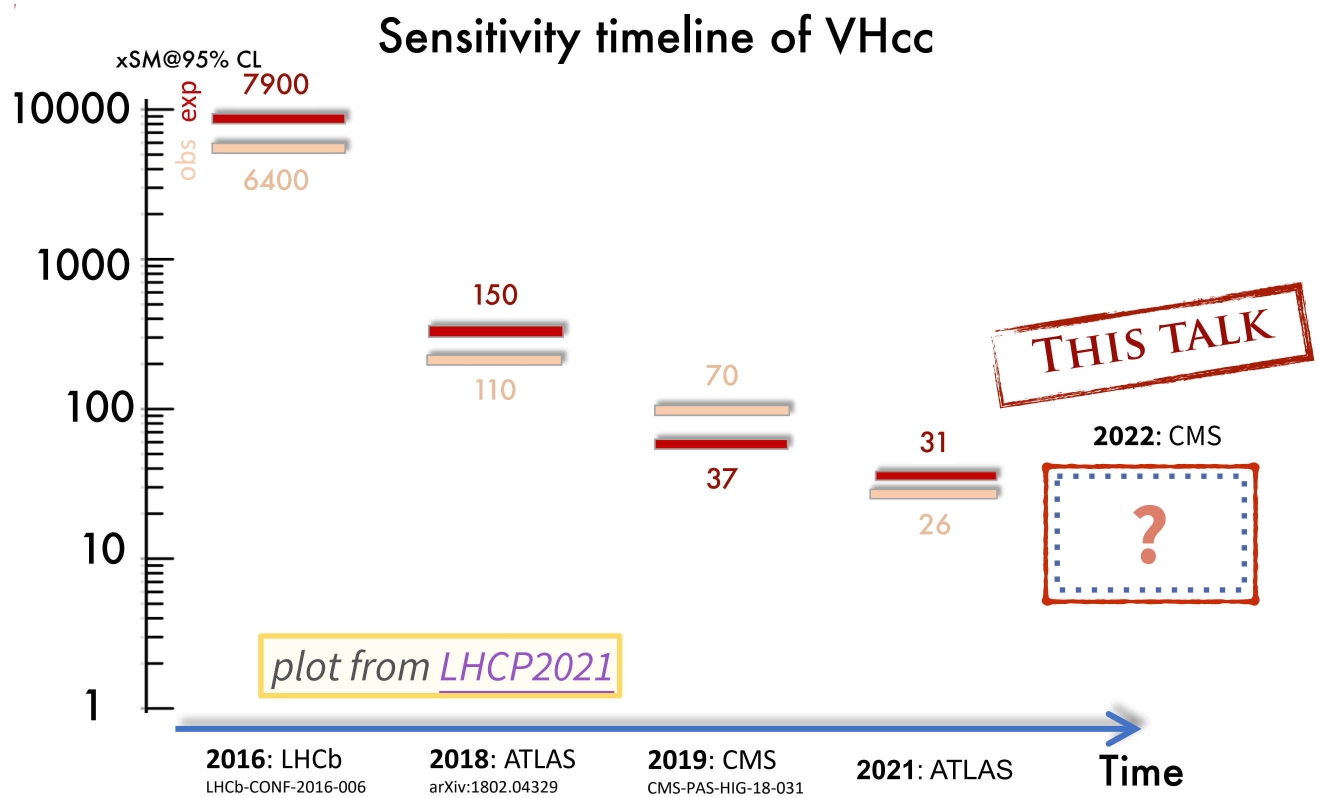


→ **VH(→cc) mode** with V= W(→ℓν) or Z(→ℓℓ/νν) is most sensitive channel by far

- leptonic decay of W/Z provides a handle to suppress multijet background

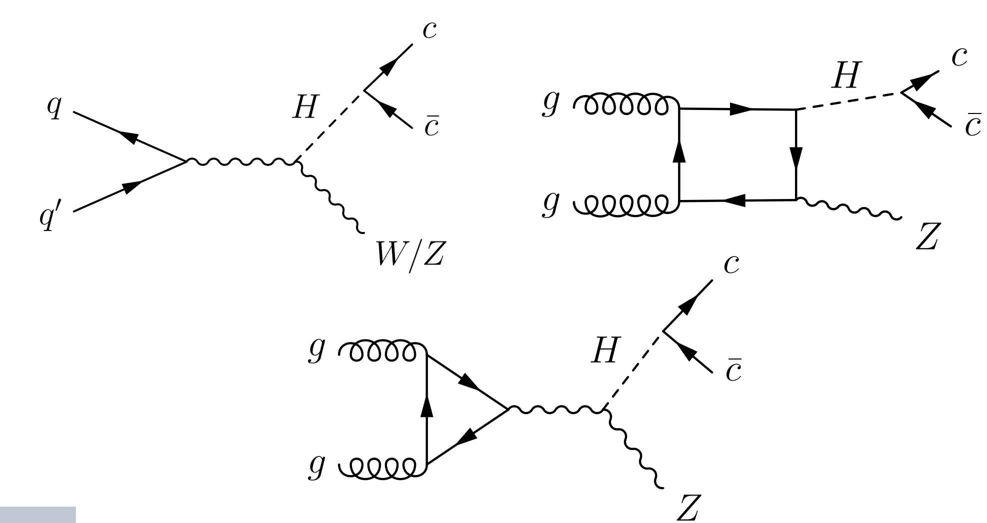


| OBS (EXP) UL σ(VHcc) | OBS (EXP) UL on κc | ∫Ldt | |
|---|---|---|---|
| μ < 110 (150) | - | 36.1 $fb^{-1}$ (2016) | ATLAS [PRL 120 (2018) 211802] Z(→ℓℓ)H |
| μ < 70 (37) | - | 35.9 $fb^{-1}$ (2016) | CMS [JHEP 03 (2020) 131] V(Z→ℓℓ, Z→νν, W→ℓν)H |
| μ < 26 (31) | $\|\kappa_c\|$ < 8.5 (12.4) | 139 $fb^{-1}$ (full Run 2) | ATLAS [HIGG-2021-12] V(Z→ℓℓ, Z→νν, W→ℓν)H |
| ? | ? | 138 $fb^{-1}$ (full Run 2) THIS TALK | CMS [arXiv:2205.05550 (accepted by PRL)] [CMS-PAS-HIG-21-008] V(Z→ℓℓ, Z→νν, W→ℓν)H |

*CMS VHcc search using 2016 data*

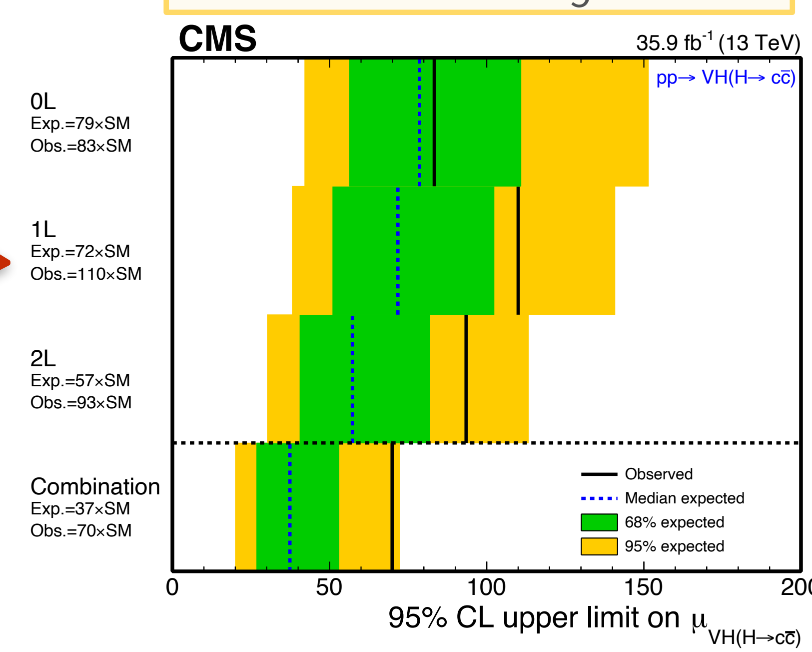

# VHcc analysis in a nutshell

NEW PHASE-SPACE EXPLORED IN CMS

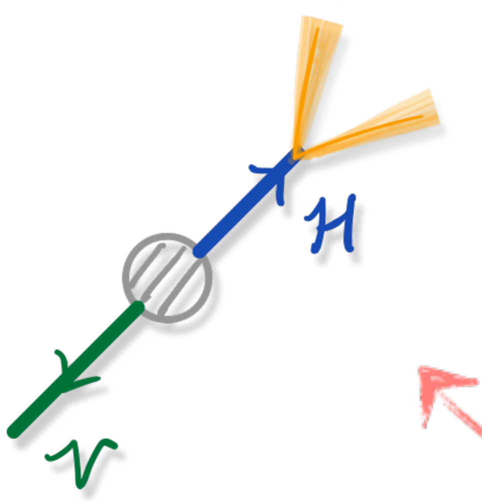


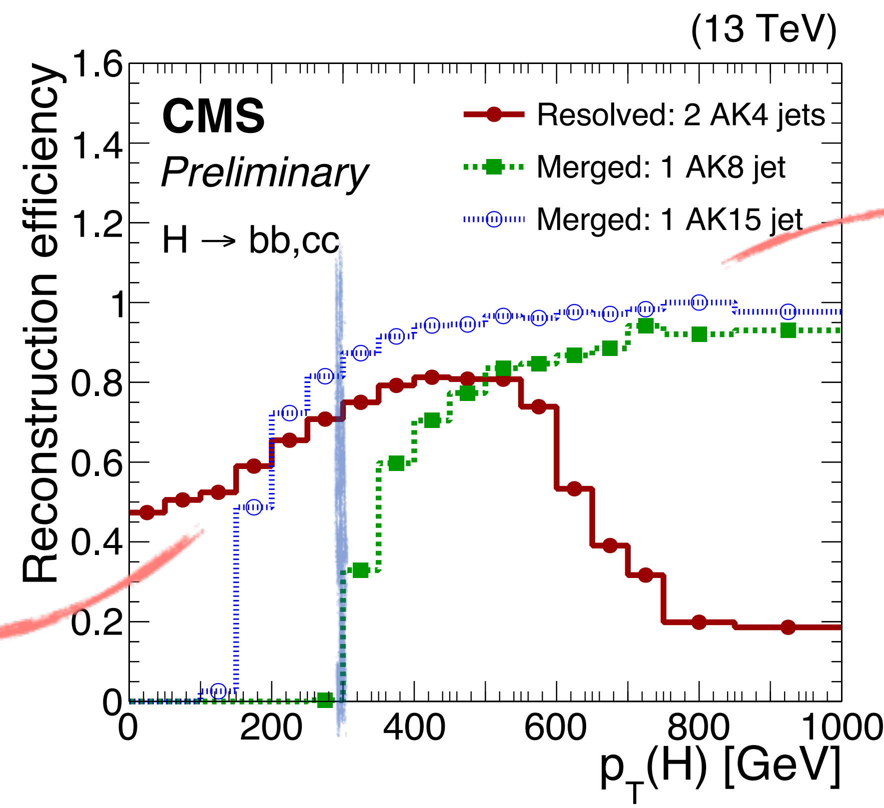


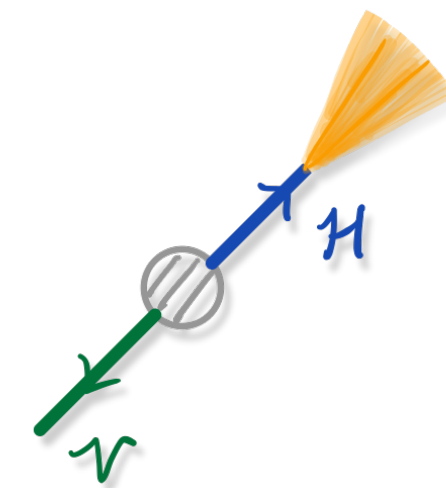


$\Delta R(c, c) \sim 2m(H)/p_T(H)$

## Resolved-jet topology

- reconstruct H→cc decay with two *R*=0.4 jets
- apply charm tagging (DeepJet) for each jet
- able to probe larger fractions of the available phase space (~95%)

## Merged-jet topology

- reconstruct H→cc decay with one large-*R* (*R*=1.5) jets
- apply di-charm tagging (ParticleNet X→cc) to the jet; able to exploit the correlations of two charms
- improved signal purity with large $p_T(H)$

# Merged-jet: H→cc identification with ParticleNet

→ Merged jet topology: Higgs candidate reconstructed by a single large-*R* jet

- using advanced deep learning approach to tag the large-*R* jet with a H→cc signature
- major improvement has been made in improving the tagger design

**JHEP 03 (2020) 131** (2016 analysis)

**DeepAK8 (DeepAK15)** [JINST 15 (2020) P06005]

- multi-class DNN classifier with 1D convolutional neural network
- directly uses jet constituents (particle-flow candidates / secondary vertices)
- mass decorrelation via adversarial training

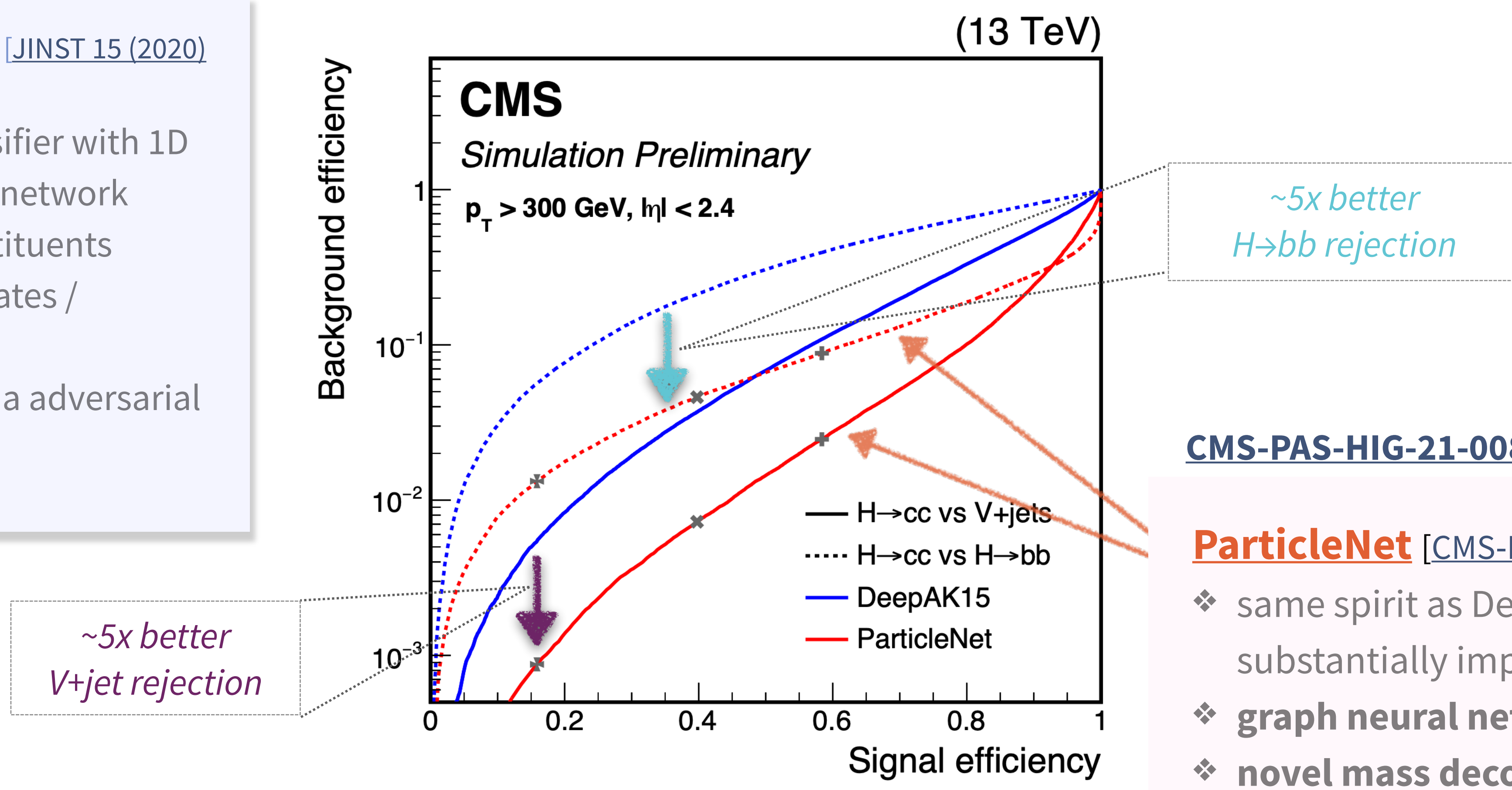


**CMS-PAS-HIG-21-008** (Run 2 analysis)

**ParticleNet** [CMS-DP-2020-002]

- same spirit as DeepAK8, but substantially improved:
- **graph neural network architecture**
- **novel mass decorrelation technique**

→ details in the next slide

# Merged-jet: ParticleNet

- ➔ ***ParticleNet***: an advanced multi-class jet classifier with a graph neural networks (**GNN**) structure, processing input features on a "**point cloud**" [CMS-DP-2020-002]
  - ❖ **point cloud:** an unordered set of particles
  - ❖ **GNN**: apply the EdgeConv operation on the point cloud
  - ❖ able to use **low-level jet features** as inputs (particle-flow candidates & secondary vertices)

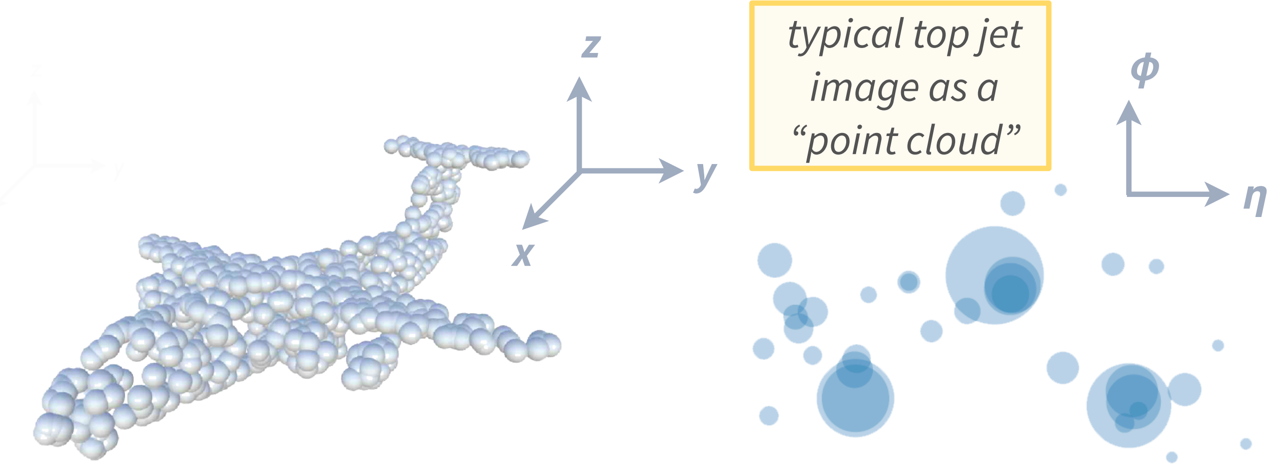


- ➔ Details and techniques:
  - ❖ **categorisation**: resonance decaying to different flavour contents & QCD:
    - X→bb, X→cc, X→qq, QCD (bb, cc, b, c, others)
  - ❖ **mass decorrelation** (decorrelate with Higgs mass): signal & QCD reweighted on a flat ($p_T$, mass) distribution before training
  - ❖ **novel calibration method**: select a phase-space from g→cc that resembles H→cc jets, by vetoing jets with large gluon contamination using a BDT [CMS-DP-2022-005]

*ParticleNet mass-decorrelation effect*

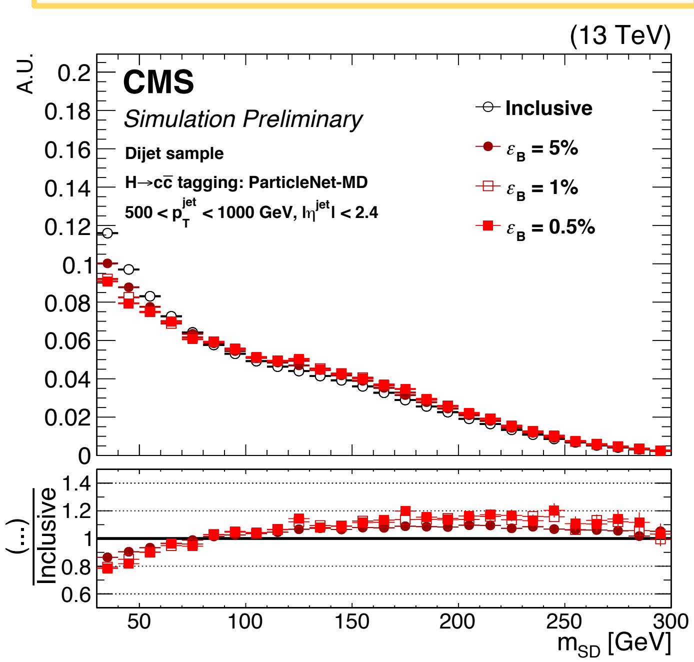


*tagger calibration: use BDT to select a phase-space from g→cc*

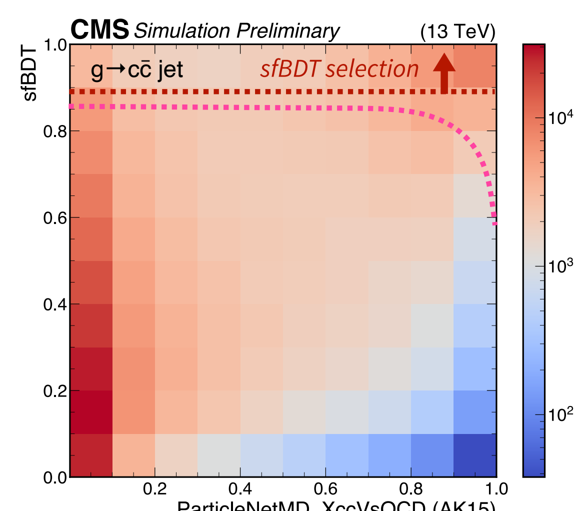


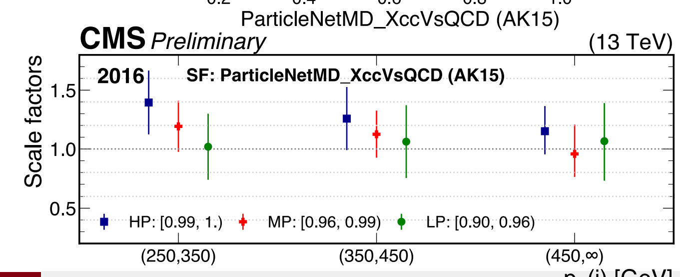

# Merged-jet: analysis techniques & strategy

➔ ParticleNet for cc-tagging on large-*R* (*R*=1.5) jets

- ✓ **huge improvement**: ~5 times increase in BKG rejection w.r.t. DeepAK15 tagger (2016) [CMS-DP-2020-002]
- ✓ tagger calibration with novel BDT approach [CMS-DP-2022-005]

➔ Di-charm jet mass regression

- ❖ use the ParticleNet architecture with a regression layer [CMS-DP-2021-017]
- ❖ ~20–25% improvement in exp. upper limit, w.r.t. using soft-drop mass

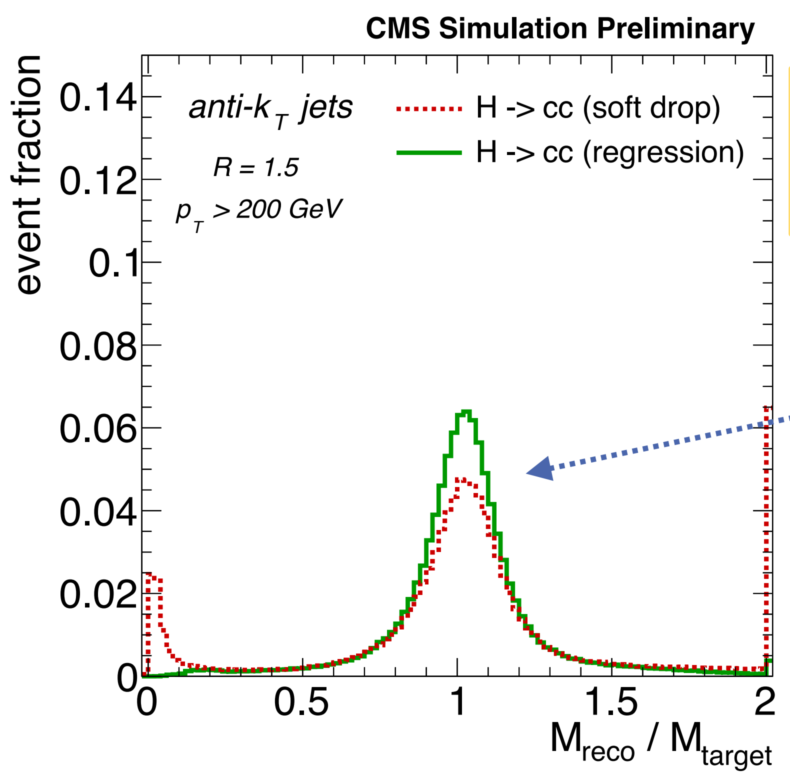


*soft-drop mass vs. regressed mass resolution*

*improved sensitivity with mass regression technique*

*Analysis strategy*

➔ train **kinematics BDTs** to separate VHcc signal vs. BKG

- ❖ using only kinematics properties - no mass/flavour information
- ❖ goal: **decorrelated BDT with $H_{cand}$ mass and ParticleNet cc-tagging discriminant**

➔ CR defined by inverting the BDT cut

- ❖ also define high $N_j$ region for $t\bar{t}$

➔ apply **cc-tagging cut on three WPs**

➔ finally extract VHcc by **fitting on the regressed mass** variable

# Merged-jet: CRs and SR

*example post-fit plots for CR and SR, for 1L W(μν)*

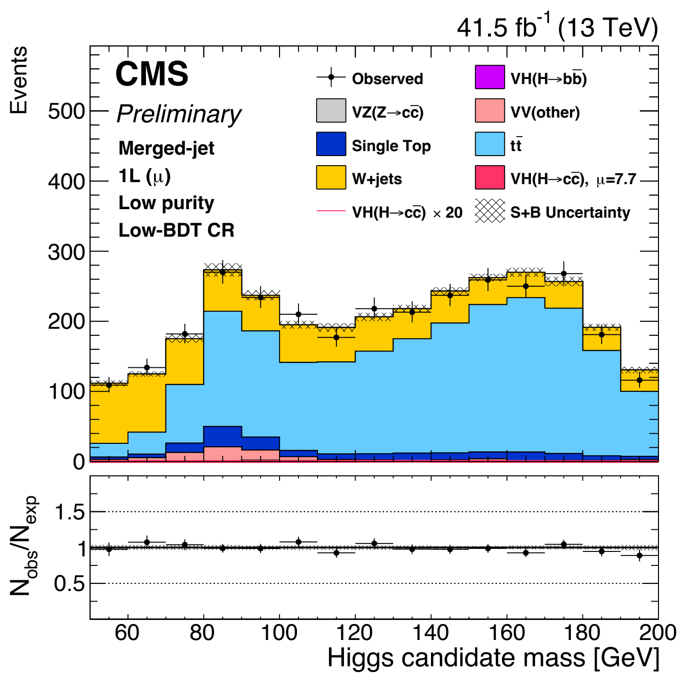


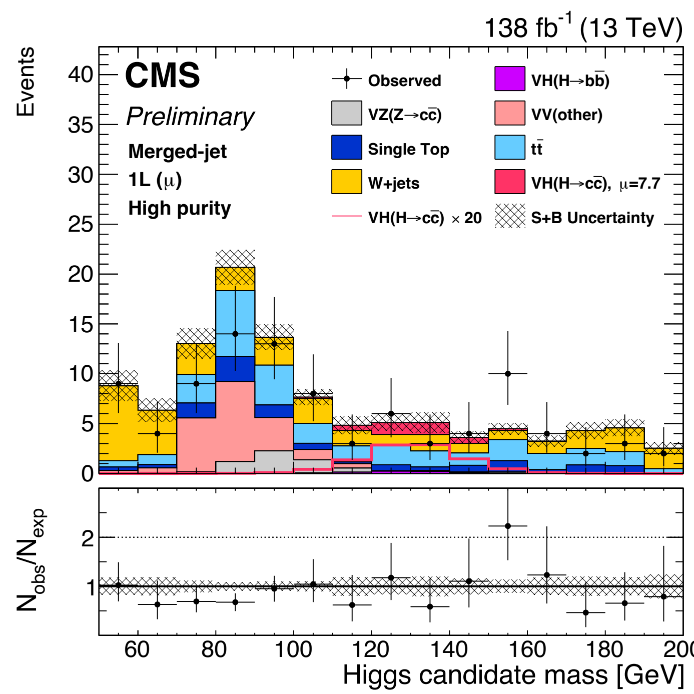


➔ Simultaneous fit of all SR and CRs

- extract BKG normalisation factors assigned to V+jets and tt̄ components

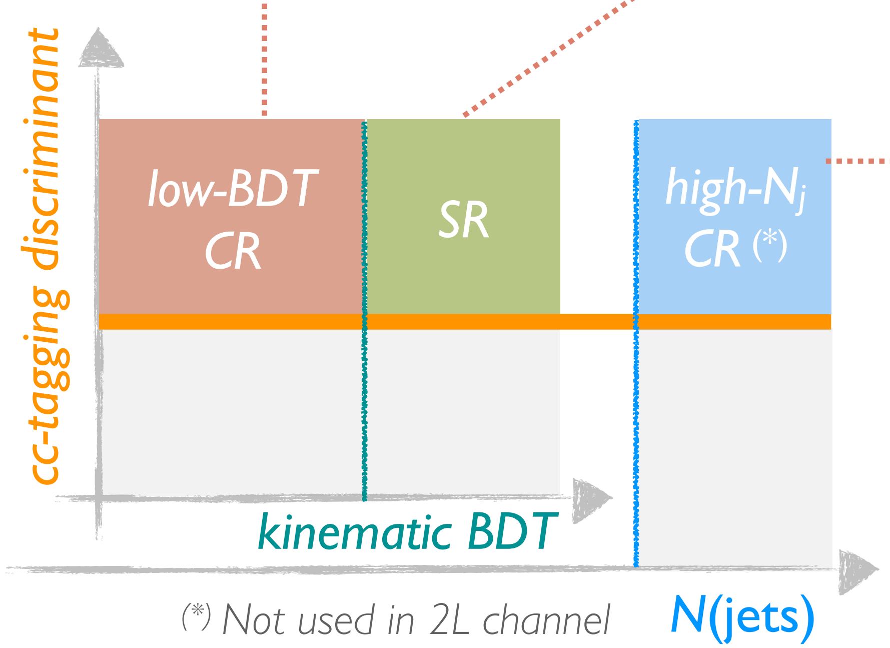


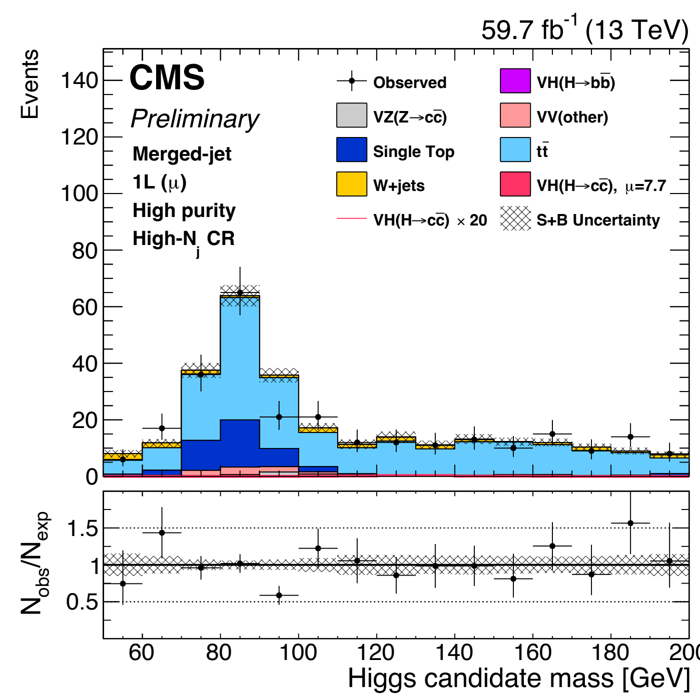


*SR and CRs definition*

# Resolved-jet: analysis techniques

→ **Charm jet identification with DeepJet algorithm** [JINST 15 (2020) P12012]

- deep neural network in CNN+RNN architecture
- two discriminants defined for c-jet vs. b-jet and c-jet vs. light-jet separation
- ~2x (40%) improvements for light (b)jet rejection at 40% c jet efficiency w.r.t. DeepCSV (2016)

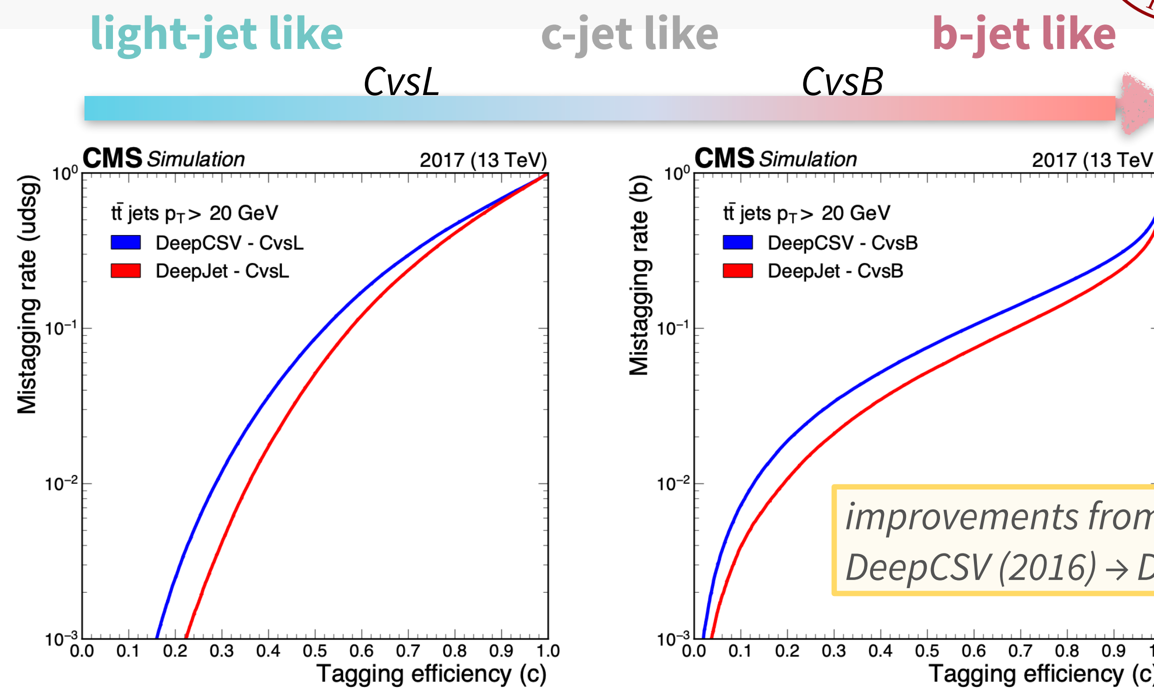


*improvements from DeepCSV (2016) → DeepJet*

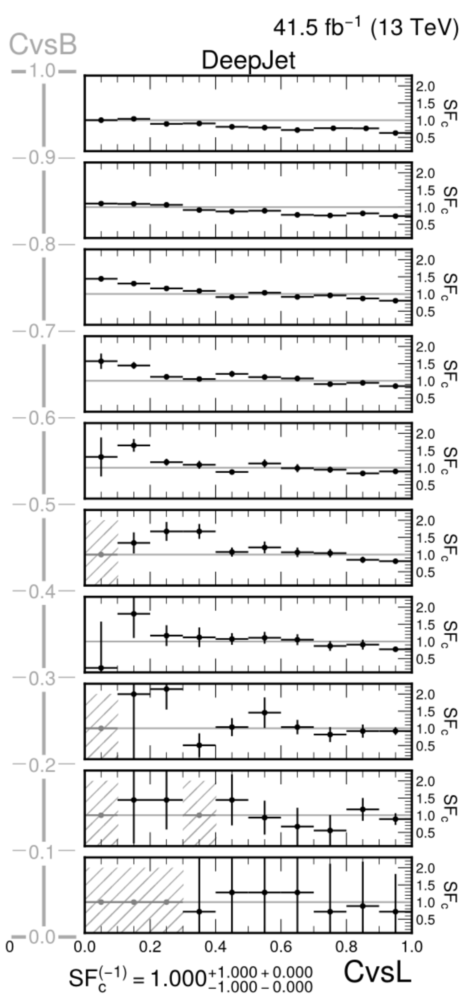


*SF for entire c-tagging shape*

*improved mass resolution on di-jet regressed mass*

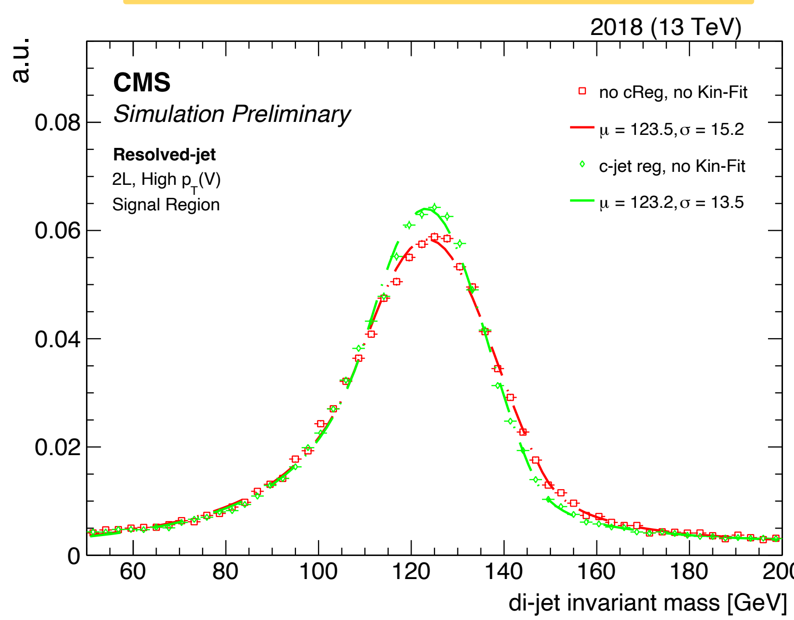


→ **Novel charm tagger shape calibration** [JINST 17 (2022) P03014]

- correct the entire distribution of the c-tagging shape
- SF derived with an iterative approach using three samples enriched in light/b/c jet

→ **Charm jet energy regression**

- regress RECO-to-GEN energy correction using DNN
- ~15% improvement in di-jet invariant mass resolution

# Resolved-jet: analysis strategy

- ➔ define SR: two jets with **high c-tagging score**
- ➔ train **BDT** to separate VHcc signal vs. backgrounds
  - ❖ **kinematic fit** used in 2L: post-fit Z(ℓℓ)H(cc) system kinematics used as BDT input
- ➔ CRs defined for V+b/c/light jets, and tt̄
  - ❖ by inverting c-tagger selection or vetoing Z/$H_{cand}$ mass / requiring additional ℓ/jet
- ➔ finally extract VHcc signal by fitting on BDT
  - ❖ **simultaneous fit** on SR (on BDT) and all CRs (on c-tagging discriminant)

*BDT to distinguish VHcc from backgrounds*

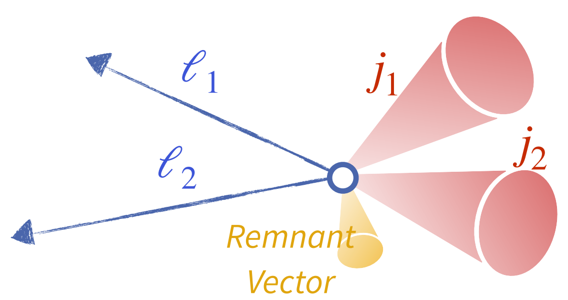


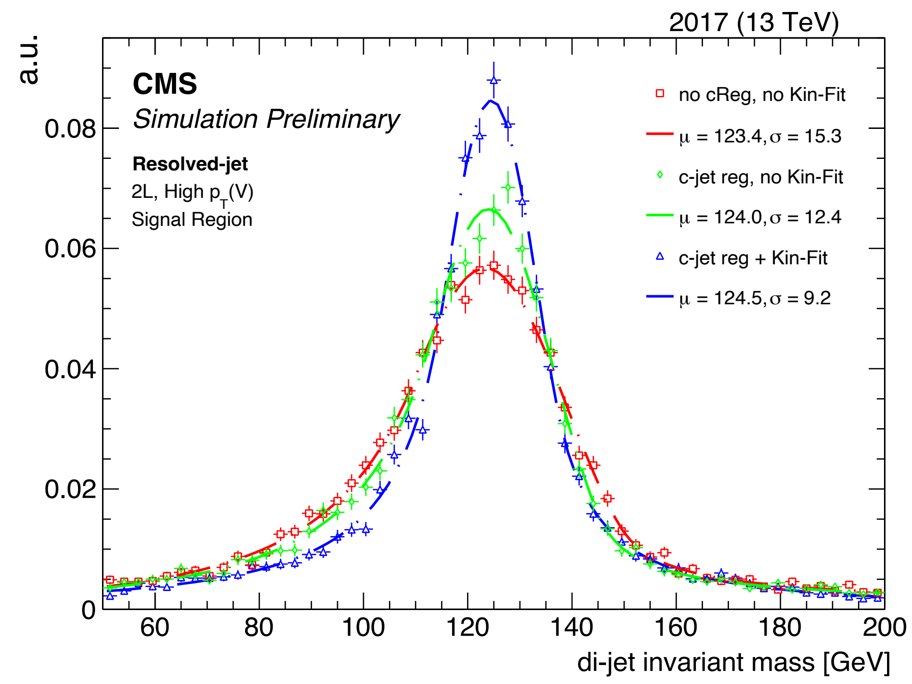


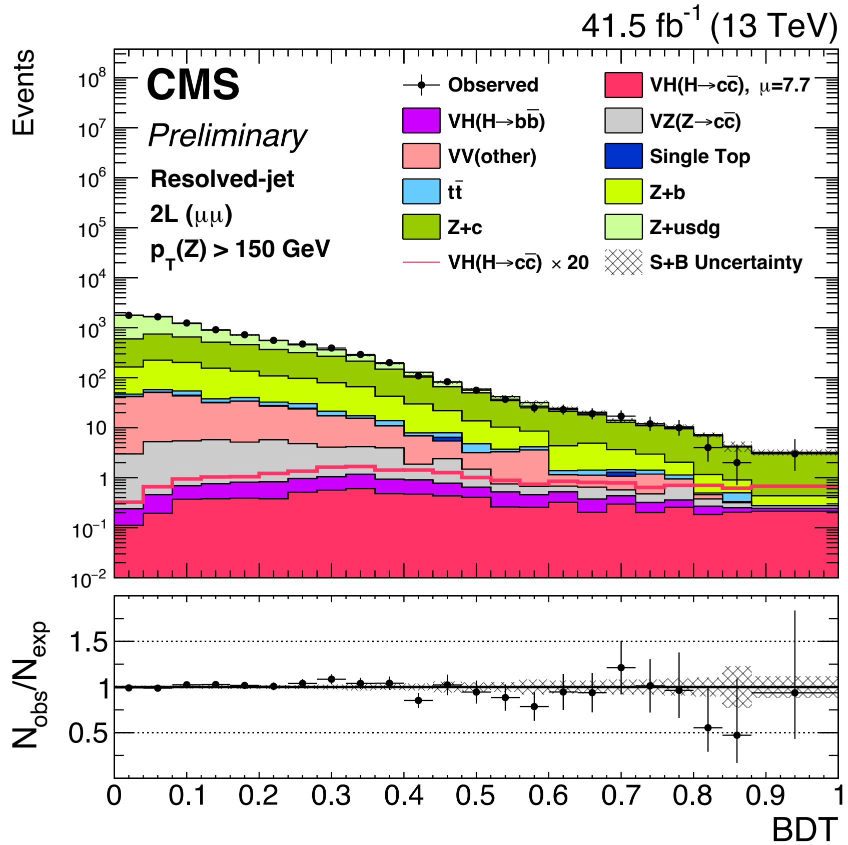

# Resolved-jet: CRs and post-fit SR

*example CR plots for 2L high-$p_T$(V) channel, year 2017*

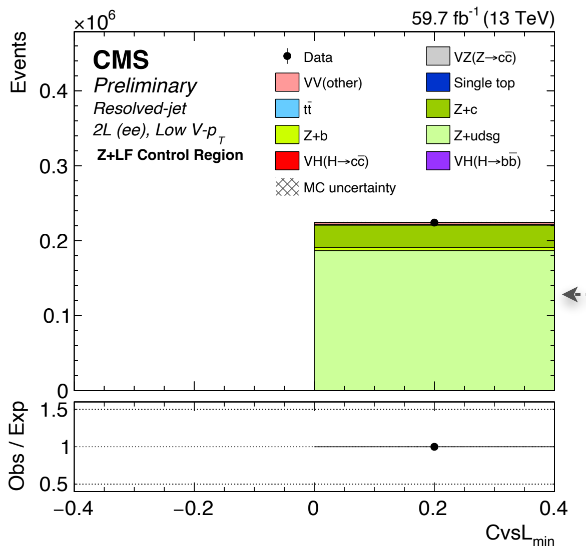


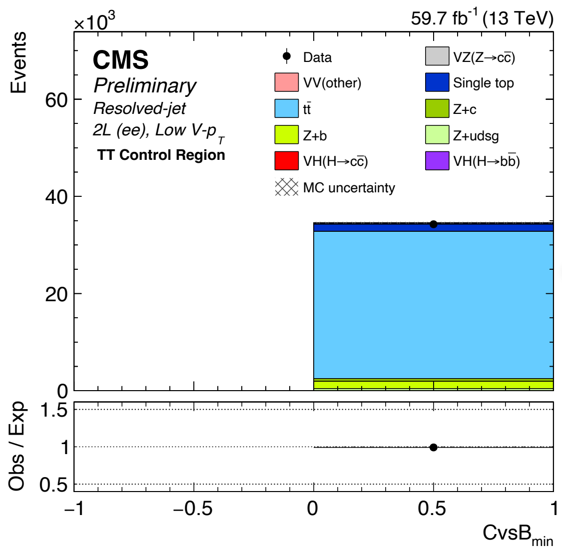


*SR and CRs definition*

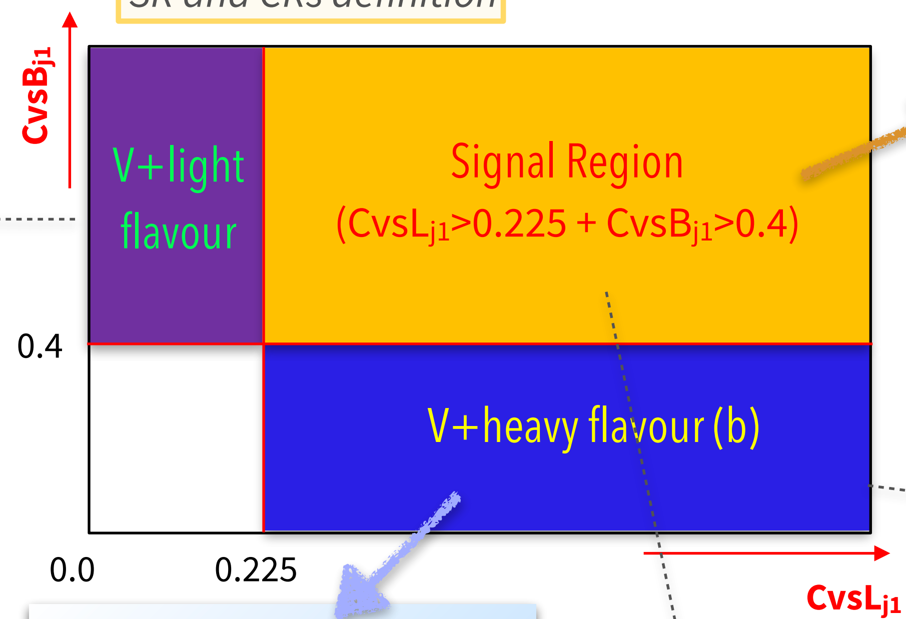


V+charm
veto the $H_{cand}$ mass region

tt̄
invert Z mass (2L)
require add. jet (1L)
require add. ℓ and jets (0L)

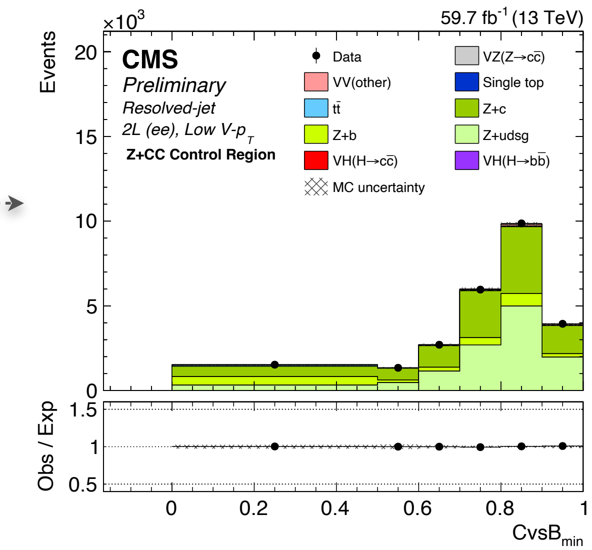


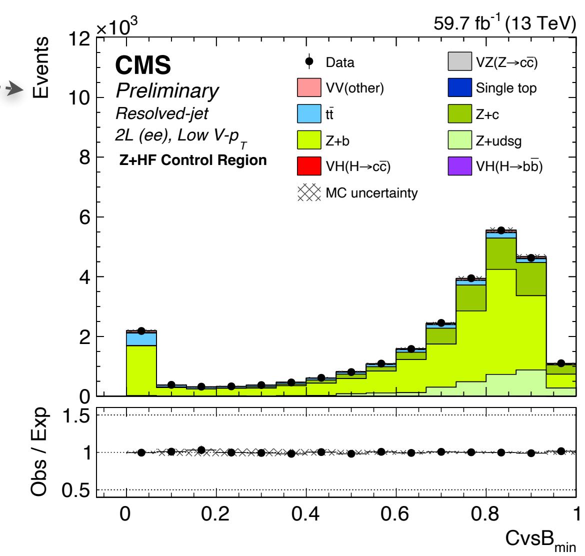


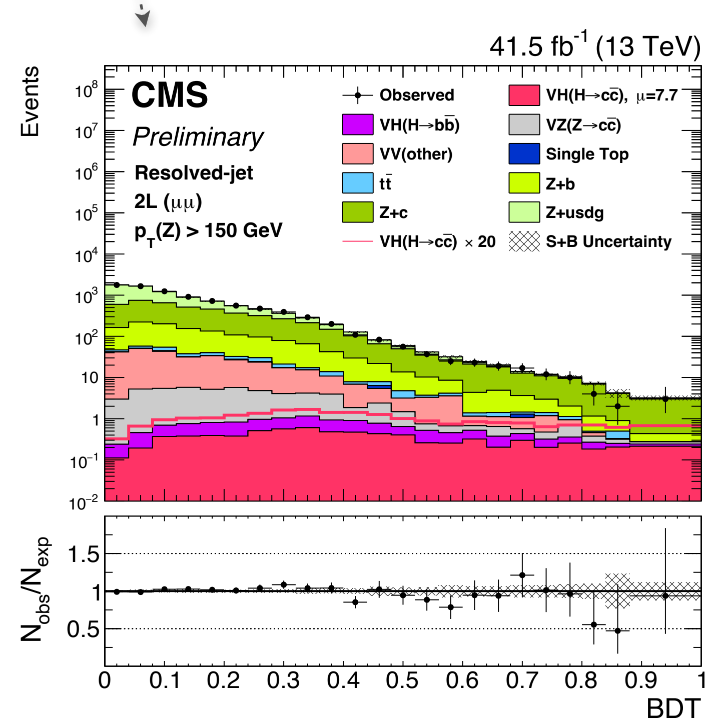


*SR plot (BKG impose norm factors extracted from CR-only fit)*

➔ Simultaneous fit in all SR and CRs

- **BKG normalisation factors** assigned to multiple components and extracted from the fit
- combined with merged-jet topology for the final signal extraction fit

# Results from VZcc validation

RESULT

- ➔ Use VZcc analysis as a validation
  - ❖ consider **VZcc process as the signal** and VHcc as the background
  - ❖ apply with the same analysis and fit strategy (for resolved-jet analysis: re-train the BDT using VZcc as the signal)

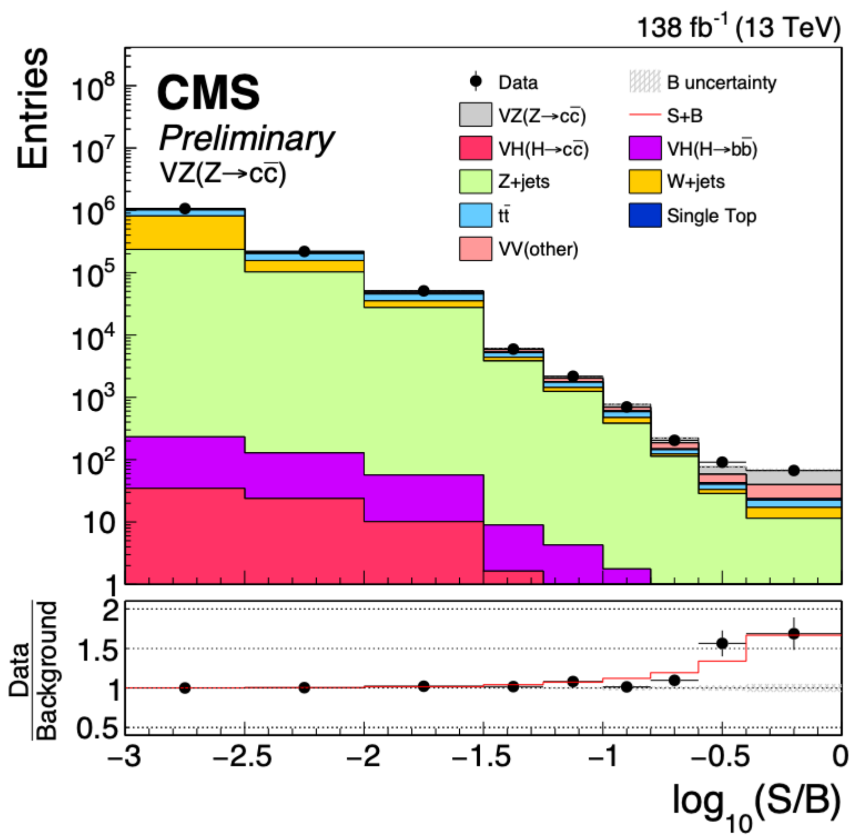


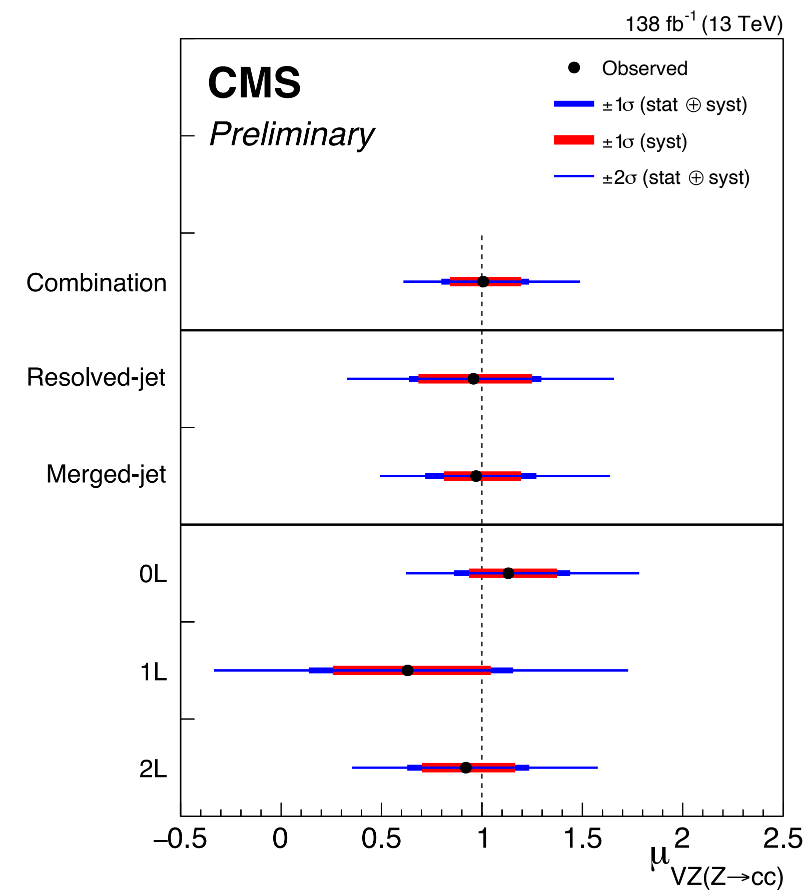


Observed significance for VZ(Z → cc): **5.7σ**

- expected significance: 5.9σ

First observation of Z→cc at a hadron collider!

Best-fit signal strength: $\mu_{VZ(Z \to cc)} = 1.01^{+0.23}_{-0.21}$

- very good agreement with SM expectation
- consistent results between topologies/channels

# VHcc results

RESULT

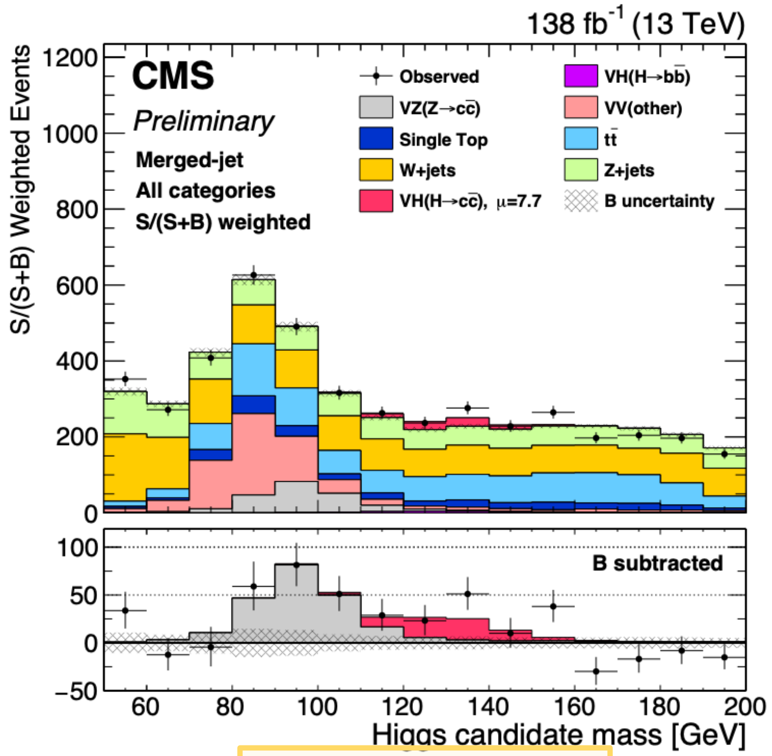


merged-jet topology

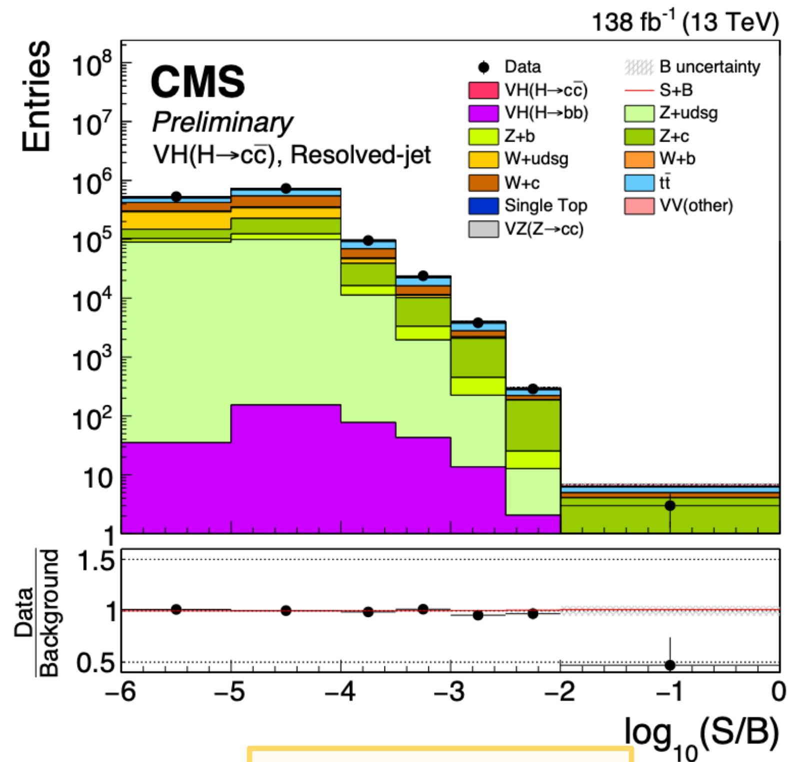


resolved-jet topology

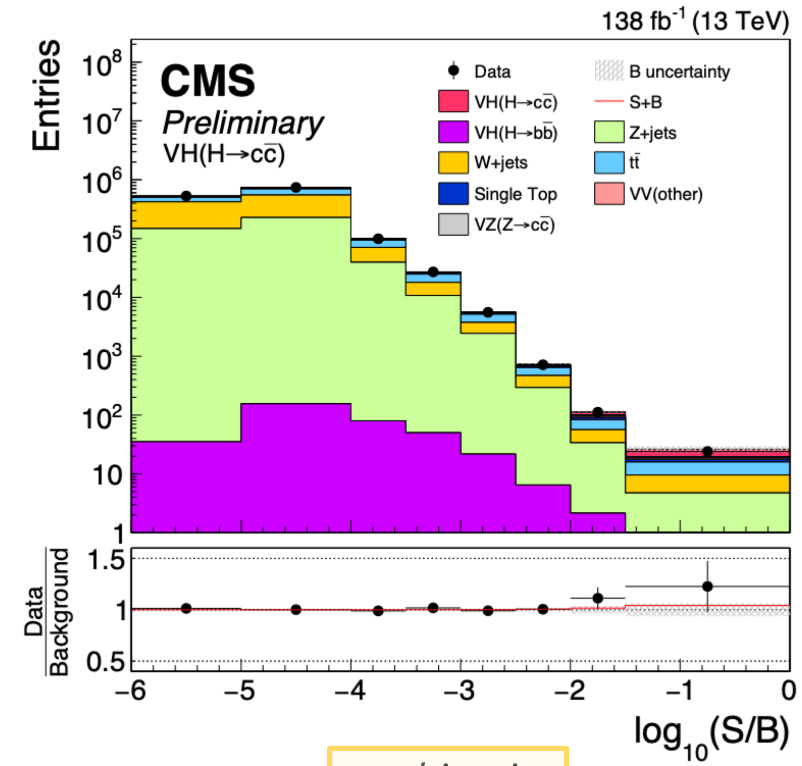


combination

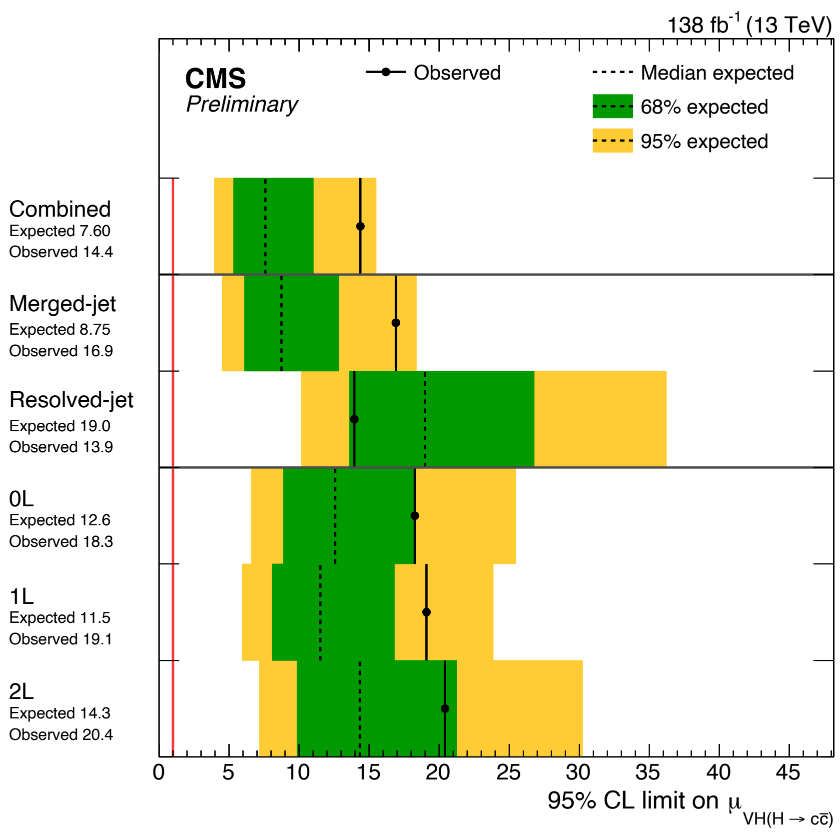


Upper limits on the VH(H → cc) signal strength at 95% CL

- **$\mu_{VH(H\to cc)}$ < 14 (7.6)** observed (expected)
- setting stronger limit w.r.t. ATLAS full Run 2 result: $\mu_{VH(H\to cc)}$ < 26 (31) obs. (exp.) [arXiv:2201.11428]

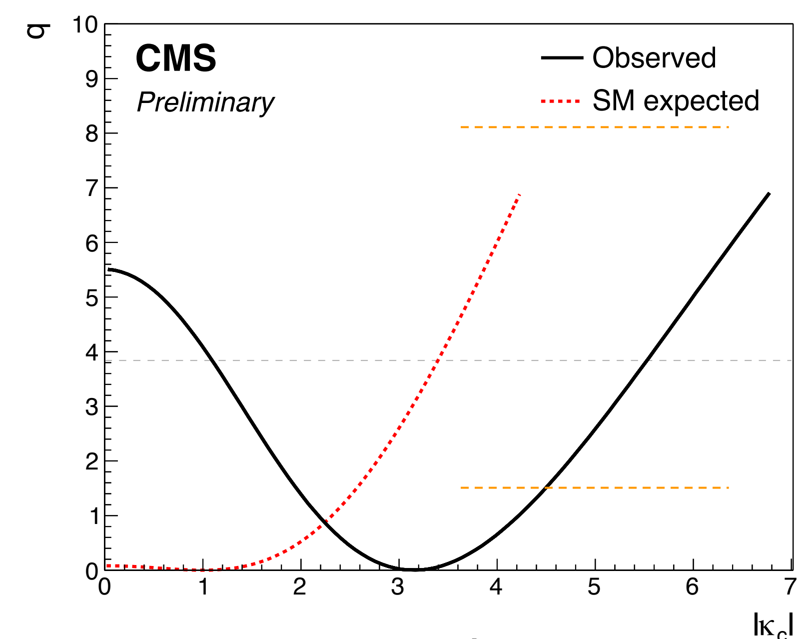


95% CL interval on $\kappa_c$:
**1.1 < $|\kappa_c|$ < 5.5 ($|\kappa_c|$ < 3.4)**
observed (expected)

# Projection at HL-LHC

➔ Strategy for **merged-jet topology** extrapolated to HL-LHC (3000 $fb^{-1}$)

- **simultaneous extraction of H→bb and H→cc signal strength**
- based on Run 2 analysis and add new categories enriched for H→bb; lower the pT threshold to 200 GeV → increase the signal acceptance

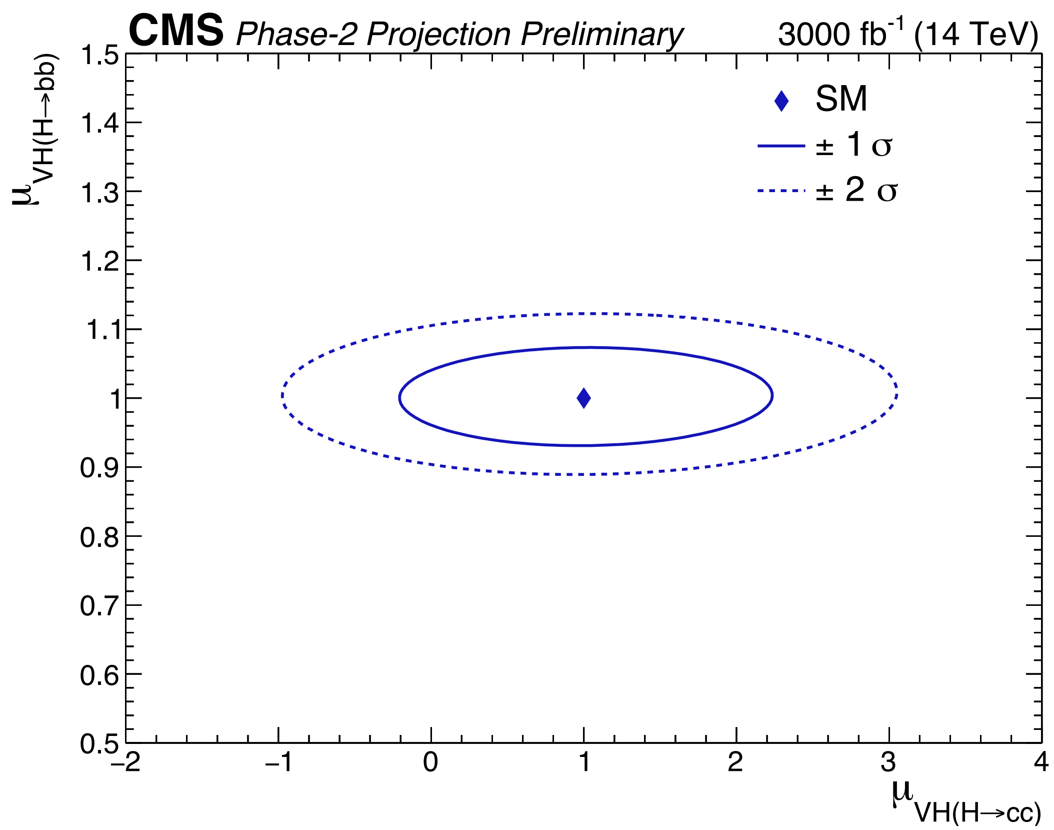


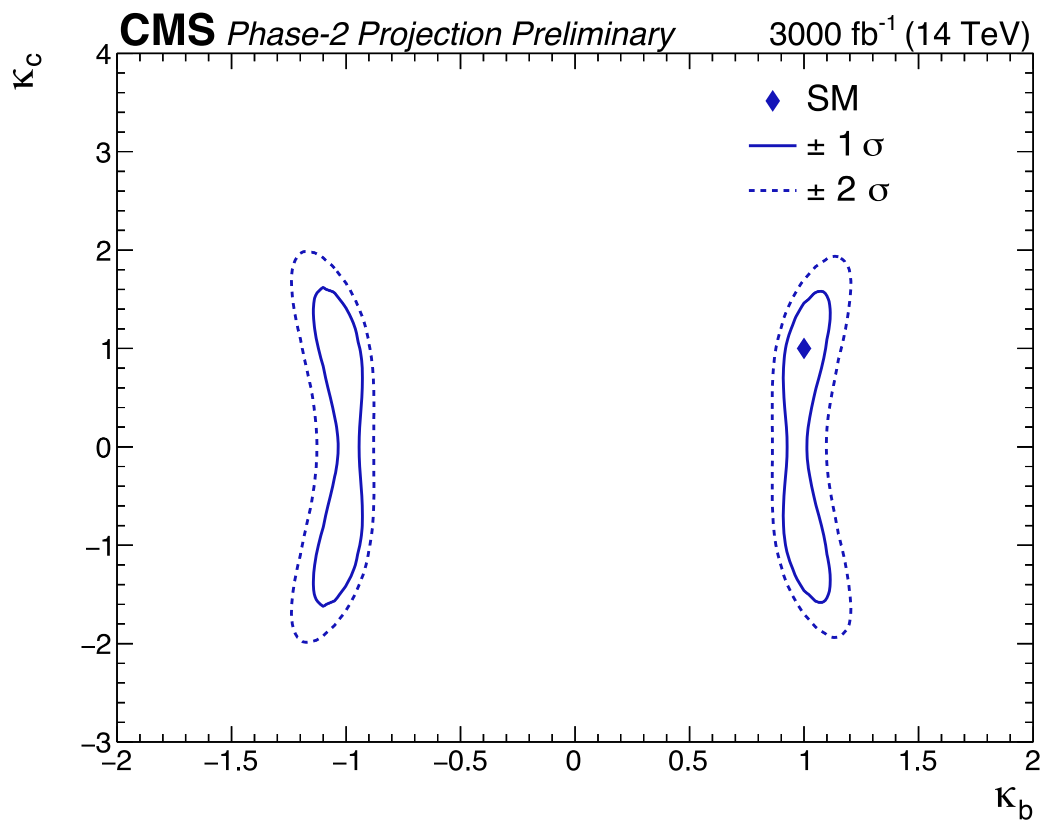


- $\mu_{VH(H\to bb)}$ = 1.00 ± 0.03 (stat.) ± 0.04 (syst.) = 1.00 ± 0.05 (total)
- $\mu_{VH(H\to cc)}$ = 1.0 ± 0.6 (stat.) ± 0.5 (syst.) = 1.0 ± 0.8 (total)

⇨ **Expected sensitivity reach ~*o*(0.1-1) level with the use of novel tagger and strategy**

# Summary

- ➔ The search of H→cc in the VH production mode using full Run 2 data is presented
  - ❖ use two complementary approaches: **resolved- & merged-jet topology** to fully explore the VH(H→cc) decay phase-space
    - results combined to further improve the sensitivity
  - ❖ exploit advanced **DNN-based charm & di-charm jet taggers**
    - **huge performance gains** in charm tagging with the new ML techniques
  - ❖ explore DNN-based method for **jet mass/energy regression**
- ➔ The full analysis procedure validated by measuring VZ(Z→cc)
  - ❖ establish the first observation of Z→cc on a hadron collider: significance at 5.7σ
  - ❖ set the most stringent limit on VH(H→cc)
    - upper limit on 95% CL: $\mu_{VH(H\to cc)} < 14$ (7.6) observed (expected)
    - pave the way to possibly a real observation of H→cc in the future

# Backup

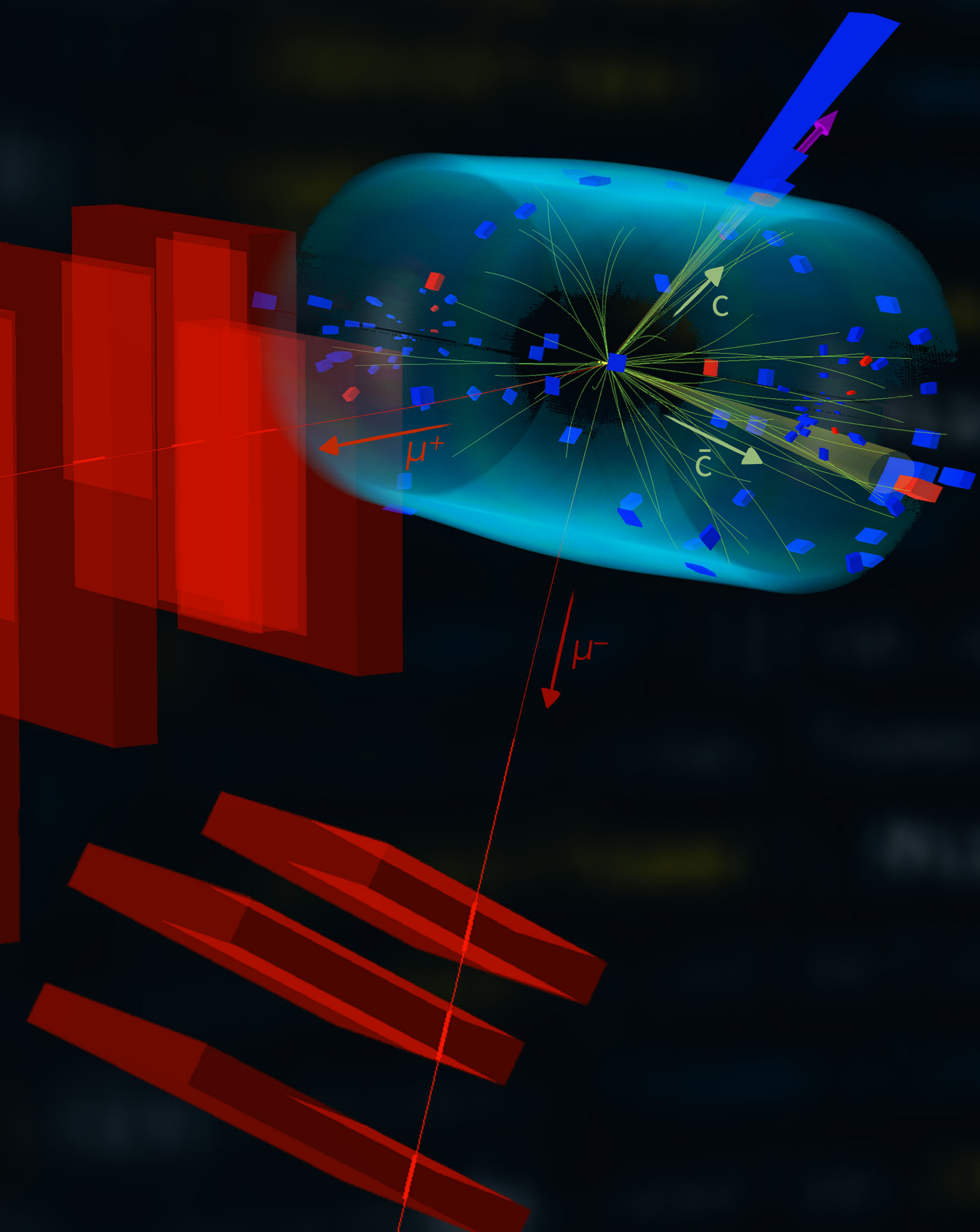

# Higgs-charm coupling at HL-LHC

→ Expected sensitivity at HL-LHC [CERN-2019-007]

| | |
|---|---|
| H→cc decay | $\lvert\kappa_c\rvert < \sim 1\text{-}2$ |
| cH production | $\lvert\kappa_c\rvert < \sim 2\text{-}3$ |
| H→J/Ψγ | $\lvert\kappa_c\rvert < \sim 80$ |
| $p_T(H)$ distribution | $\lvert\kappa_c\rvert < \sim 10$ |
| WH charge assymetry | $\lvert\kappa_c\rvert < \sim 4\text{-}5$ |

# ATLAS HL-LHC projection for H→cc

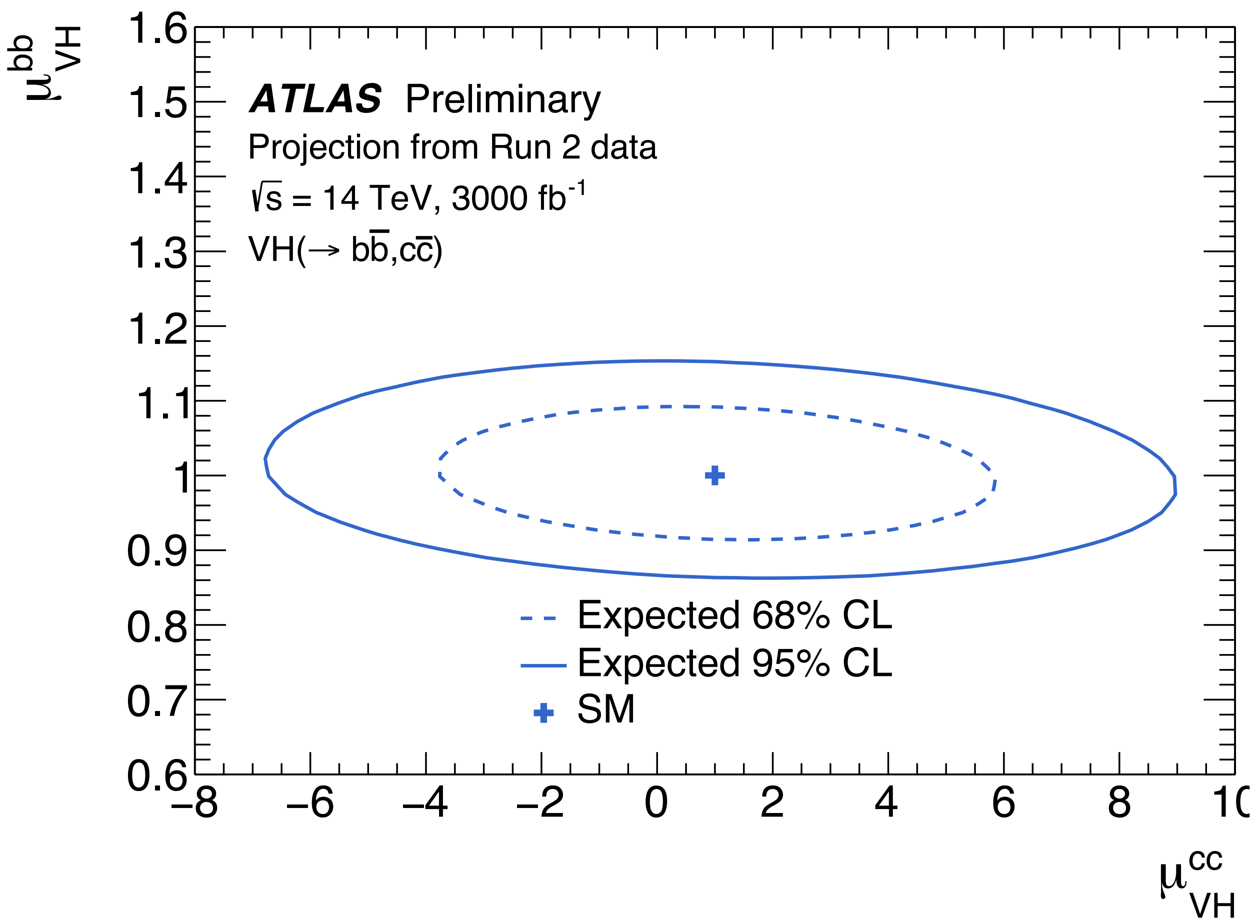


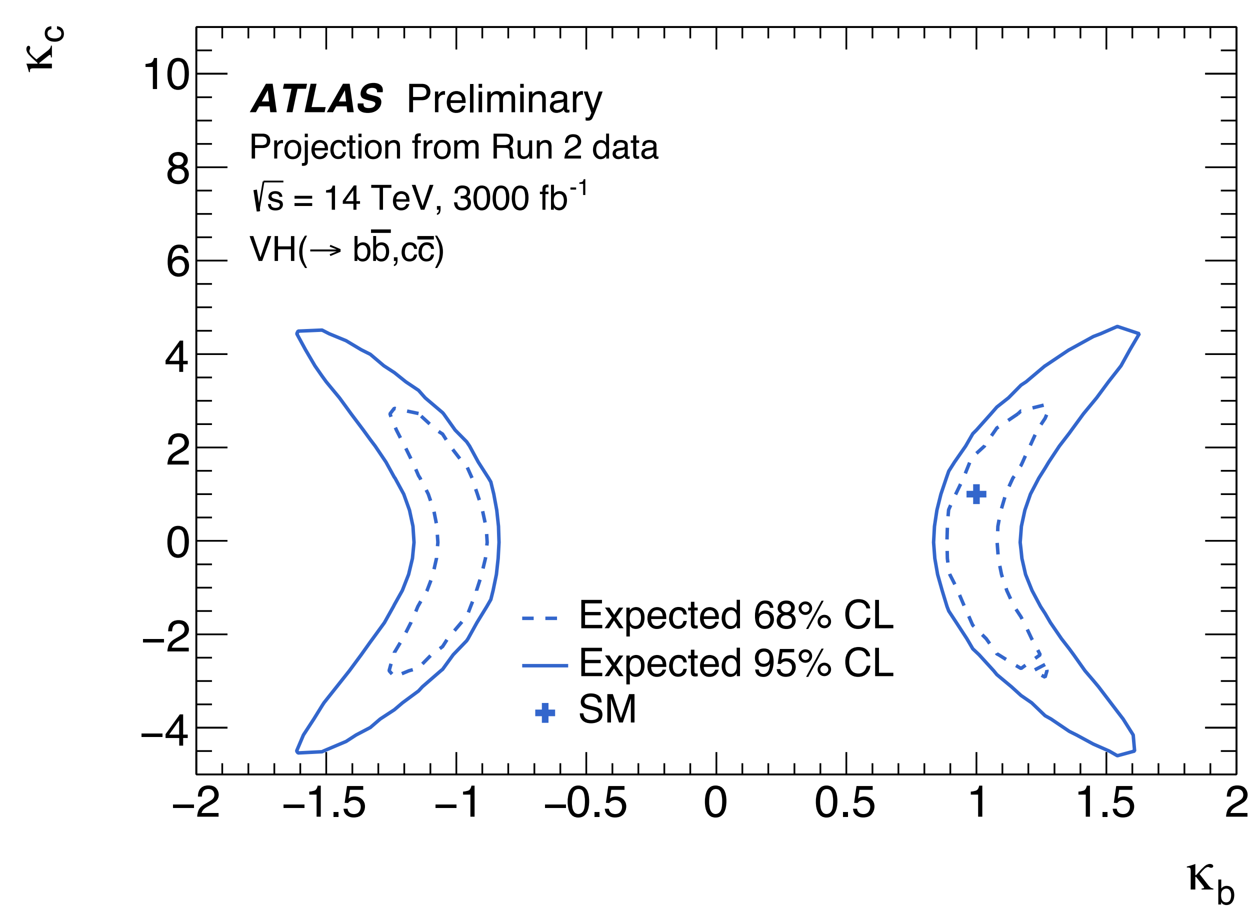

# Baseline event selection

*Merged-jet topology*

| Variable | 0L | 1L | 2L |
|---|---|---|---|
| $p_T^\ell$ | — | (>25,>30) | >20 |
| Lepton isolation | — | (<0.06, —) | (<0.25, —) |
| $N_{a\ell}$ | =0 | =0 | — |
| $M(\ell\ell)$ | — | — | 75–105 |
| $N^{aj}_{small\text{-}R}$ | <2 | <2 | <3 |
| $p_T^{miss}$ | >200 | >60 | — |
| $p_T(V)$ | >200 | >150 | >150 |
| $p_T(H_{cand})$ | >300 | >300 | >300 |
| $m\,(H_{cand})$ | 50–200 | 50–200 | 50–200 |
| $\Delta\phi(V, H_{cand})$ | >2.5 | >2.5 | >2.5 |
| $\Delta\phi(\vec{p}_T^{miss}, j)$ | >0.5 | — | — |
| $\Delta\phi(\vec{p}_T^{miss}, \ell)$ | — | <1.5 | — |
| Kinematic BDT | >0.55 | 0.55–0.7, >0.7 | >0.55 |
| $c\bar{c}$ discriminant | | | |
| High purity | >0.99 | >0.99 | >0.99 |
| Medium purity | 0.96–0.99 | 0.96–0.99 | 0.96–0.99 |
| Low purity | 0.90–0.96 | 0.90–0.96 | 0.90–0.96 |

*Resolved-jet topology*

| Variable | 0L | 1L | 2L low-$p_T(V)$ | 2L high-$p_T(V)$ |
|---|---|---|---|---|
| $p_T^\ell$ | — | (>25,>30) | >20 | >20 |
| Lepton isolation | — | (<0.06, —) | (<0.25, —) | (<0.25, —) |
| $N_{a\ell}$ | =0 | =0 | — | — |
| $M(\ell\ell)$ | — | — | 75–105 | 75–105 |
| $p_T(j_1)$ | >60 | >25 | >20 | >20 |
| $p_T(j_2)$ | >35 | >25 | >20 | >20 |
| $CvsL(j_1)$ | >0.225 | >0.225 | >0.225 | >0.225 |
| $CvsB(j_2)$ | >0.4 | >0.4 | >0.4 | >0.4 |
| $N^{aj}_{small\text{-}R}$ | — | <2 | — | — |
| $p_T^{miss}$ | > 170 | — | — | — |
| $p_T^{miss}$ significance | — | >4 | — | — |
| $p_T(V)$ | >170 | >100 | 60–150 | >150 |
| $p_T(H_{cand})$ | >120 | >100 | — | — |
| $m\,(H_{cand})$ | <250 | <250 | <250 | <250 |
| $\Delta\phi(V, H_{cand})$ | >2.0 | >2.5 | >2.5 | >2.5 |
| $\Delta\phi(\vec{p}_T^{miss}, j)$ | >0.5 | — | — | — |
| $\Delta\phi(\vec{p}_T^{miss}, \ell)$ | — | <2.0 | — | — |

# Uncertainties

*Merged-jet topology*

| Uncertainty source | $\Delta\mu / (\Delta\mu)_{tot}$ |
|---|---|
| **Statistical** | **88%** |
| Background normalizations | 39% |
| **Experimental** | **40%** |
| Sizes of the simulated samples | 24% |
| Charm identification efficiencies | 26% |
| Jet energy scale and resolution | 15% |
| Simulation modeling | 1% |
| Luminosity | 5% |
| Lepton identification efficiencies | 2% |
| **Theory** | **25%** |
| Backgrounds | 21% |
| Signal | 14% |

*Resolved-jet topology*

| Uncertainty source | $\Delta\mu / (\Delta\mu)_{tot}$ |
|---|---|
| **Statistical** | **66%** |
| Background normalizations | 28% |
| **Experimental** | **72%** |
| Sizes of the simulated samples | 59% |
| Charm identification efficiencies | 27% |
| Jet energy scale and resolution | 17% |
| Simulation modeling | 20% |
| Luminosity | 13% |
| Lepton identification efficiencies | 10% |
| **Theory** | **22%** |
| Backgrounds | 21% |
| Signal | 7% |

# Datasets and MC samples

- Datasets and triggers
  - 138 $fb^{-1}$ for full Run 2 data
  - **0L**: MET dataset + MET_MHT triggers
  - **1L**: SingleElectron/SingleMuon dataset + single-e/μ triggers
  - **2L**: DoubleEG/DoubleMuon dataset + double-e/μ triggers
    - (merged-jet analysis uses single-e/μ datasets and triggers)
- Simulated samples
  - **W/Z+jets**: MadGraph5 NLO samples
  - **$t\bar{t}$**: POWHEG NLO sample
  - **single top**: POWHEG/MadGraph5 NLO samples
  - **VV**: POWHEG/MadGraph5 NLO samples (NNLO QCD & NLO EW correction on $p_T(V_2)$)
  - **VH signals**: POWHEG NLO samples (NLO EWK $p_T(V)$ correction; NNLO cross section)
- Corrections
  - lepton efficiencies, JEC/JER, pileup reweighting, MET filters, c-tagging, etc.

Resolved

# DeepJet details

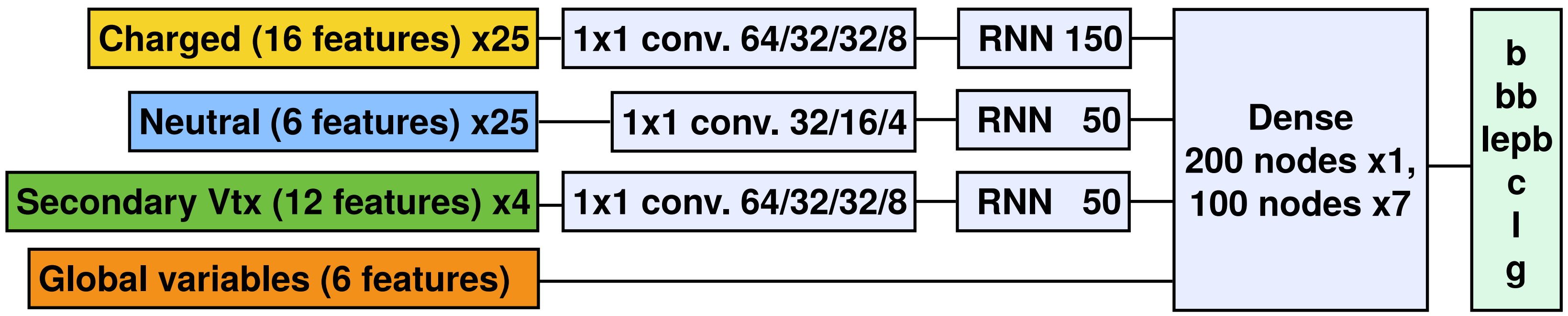


*DeepJet architecture*
*[JINST 15 (2020) P12012]*

- ➔ Use low-level features (PF candidates, SV) as well as global features
- ➔ Model architecture:
  - ❖ separate 1D CNNs to process three low-level feature classes
    - ‣ for each class, concatenate multiple CNNs with decreasing dimensions
    - ‣ compress the features to lower dimensional space
  - ❖ RNNs (LSTM type) applied after CNNs
    - ‣ better handles the variable length sequence (PF candidates/SV)
  - ❖ fully connected layer to connect all channels
- ➔ Output score:
  - ❖ 6 raw scores: bb, b (hadronically decay B-hadron), $b_{lep}$ (leptonically decay B-hadron), c, light (uds), gluon
  - ❖ construct CvsB, CvsB used in VHcc analysis

*DeepJet discriminant*

| | BvsC/L | CvsB | CvsL |
|---|---|---|---|
| DeepJet: | $P(b)+P(bb)+P(b_{lep})$ | $\frac{P(c)}{P(c)+P(b)+P(bb)+P(b_{lep})}$ | $\frac{P(c)}{P(c)+P(uds)+P(g)}$ |

Resolved

# DeepJet performance

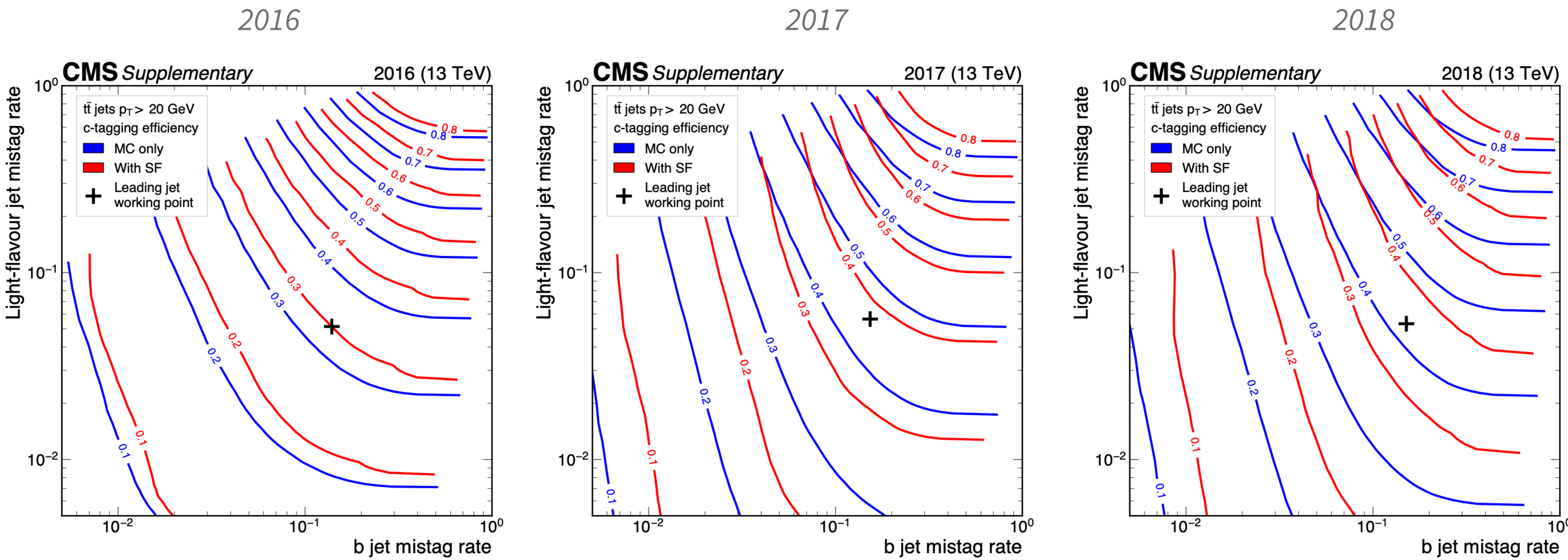


- ➔ CMS c-tagging WP: ~40% (c), ~16% (b), ~4% (light)
- ➔ ATLAS c-tagging WP: ~27% (c), 8% (b), 1.6% (light) [arXiv:2201.11428]

Resolved

# Charm tagging calibration

- ➔ Per-jet SFs derived as a 3D function of CvsL score, CvsB score, and 3 true flavours
  - ❖ 3 selections pure in b, c, and light jets
  - ❖ iteratively fit in 3 selected phase-space to find simultaneous corrections for all 3 flavours
    - Z(ℓℓ) + jets (light jet enriched)
    - W + c (c-jet enriched)
    - tt̄ (b-jet enriched)
- ➔ Propagate to analysis
  - ❖ per-event weight calculated as ***products*** of $SF_i$(flavour, CvsL, CvsB) for all jet $i$

DeepJet SFs for year 2017 JINST 17 (2022) P03014

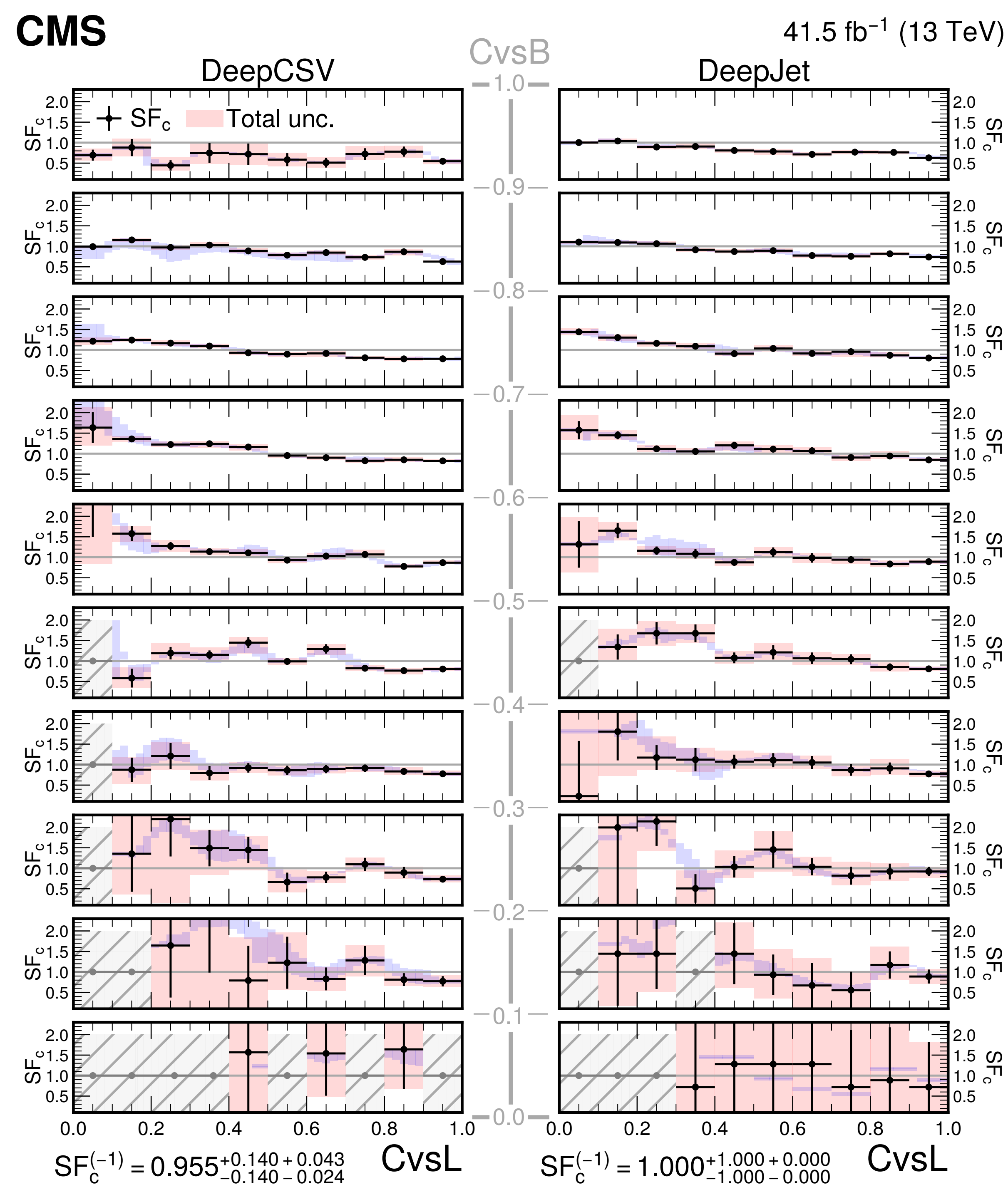

# Kinematic fit & signal extraction BDT for resolved-jet

➔ Kinematic fit (KinFit) in 2L channel

- to achieve more precise jet $p_T$ measurement and improve Higgs mass resolution by 30%

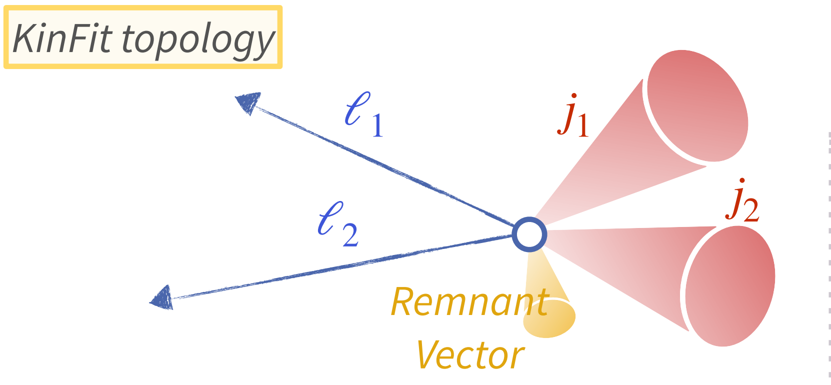


- apply the fit by:
  - constrain di-lepton system to Z mass
  - balance the $\ell\ell$+cc system in ($p_x$, $p_y$) plane
  - allow $p_{T,j1,2}$ to adjust within the uncertainties
  - add recoil jets in the $p_T$-constraint if they are present

➔ BDTs are trained in 4 categories, 3 years separately to discriminate VHcc signal vs. backgrounds

- to maximize the sensitivity
- **BDT used as the fit variable** in SR to extract the VHcc signal

BDT training variables

| | Variable | Description | 0L | 1L | 2L |
|---|---|---|---|---|---|
| Higgs and vector boson properties | $m(\mathrm{H})$ | H mass | ✓ | ✓ | ✓ |
| | $p_T(\mathrm{H})$ | H transverse momentum | — | ✓ | ✓ |
| | $p_T(\mathrm{V})$ | vector boson transverse momentum | — | ✓ | ✓ |
| | $m_T(\mathrm{V})$ | vector boson transverse mass | — | ✓ | — |
| | $p_T^{miss}$ | missing transverse momentum | ✓ | ✓ | — |
| | $p_T(\mathrm{V})/p_T(\mathrm{H})$ | ratio between vector boson and H transverse momenta | ✓ | ✓ | ✓ |
| c-tagging score | $CvsL_{max}$ | *CvsL* value of the leading *CvsL* jet | ✓ | ✓ | ✓ |
| | $CvsB_{max}$ | *CvsB* value of the leading *CvsL* jet | ✓ | ✓ | ✓ |
| | $CvsL_{min}$ | *CvsL* value of the subleading *CvsL* jet | ✓ | ✓ | ✓ |
| | $CvsB_{min}$ | *CvsB* value of the subleading *CvsL* jet | ✓ | ✓ | ✓ |
| event kinematics | $p_{Tmax}$ | $p_T$ of the leading *CvsL* jet | ✓ | ✓ | ✓ |
| | $p_{Tmin}$ | $p_T$ of the subleading *CvsL* jet | ✓ | ✓ | ✓ |
| | $\Delta\phi(\mathrm{V,H})$ | azimuthal angle between vector boson and H | ✓ | ✓ | ✓ |
| | $\Delta R(\mathrm{j_1,j_2})$ | $\Delta R$ between leading and subleading *CvsL* jets | — | ✓ | ✓ |
| | $\Delta\phi(\mathrm{j_1,j_2})$ | azimuthal angle between leading and subleading *CvsL* jets | ✓ | ✓ | — |
| | $\Delta\eta(\mathrm{j_1,j_2})$ | difference in pseudorapidity between leading and subleading *CvsL* jets | ✓ | ✓ | ✓ |
| | $\Delta\phi(\ell_1,\ell_2)$ | azimuthal angle between leading and subleading $p_T$ leptons | — | — | ✓ |
| | $\Delta\eta(\ell_1,\ell_2)$ | difference in pseudorapidity between leading and subleading $p_T$ leptons | — | — | ✓ |
| | $\Delta\phi(\ell_1,\mathrm{j_1})$ | azimuthal angle between leading $p_T$ lepton and leading *CvsL* jet | — | ✓ | — |
| | $\Delta\phi(\ell_2,\mathrm{j_1})$ | azimuthal angle between subleading $p_T$ lepton and leading *CvsL* jet | — | — | ✓ |
| | $\Delta\phi(\ell_2,\mathrm{j_2})$ | azimuthal angle between subleading $p_T$ lepton and subleading *CvsL* jet | — | — | ✓ |
| | $\Delta\phi(\ell_1,p_T^{miss})$ | azimuthal angle between leading $p_T$ lepton and missing transverse momentum | — | ✓ | — |
| | $\sigma_{cReg}(\mathrm{j_1})$ | leading $p_T$ jet resolution from c-jet energy regression | ✓ | ✓ | ✓ |
| | $\sigma_{cReg}(\mathrm{j_2})$ | subleading $p_T$ jet resolution from c-jet energy regression | ✓ | ✓ | ✓ |
| Variables from KinFit (for 2L only) | $\Delta\eta(\mathrm{V,H})\|_{kinfit}$ | difference in pseudorapidity between vector boson and H, after kinematic-fit | — | — | ✓ |
| | $\Delta\phi(\mathrm{V,H})\|_{kinfit}$ | azimuthal angle between vector boson and H, after kinematic-fit | — | — | ✓ |
| | $m(\mathrm{H})\|_{kinfit}$ | H mass after kinematic-fit | — | — | ✓ |
| | $p_T(\mathrm{H})\|_{kinfit}$ | H transverse momentum after kinematic-fit | — | — | ✓ |
| | $p_{Tmax}\|_{kinfit}$ | $p_T$ of the leading *CvsL* jet after kinematic-fit | — | — | ✓ |
| | $p_{Tmin}\|_{kinfit}$ | $p_T$ of the subleading *CvsL* jet after kinematic-fit | — | — | ✓ |
| | $p_T(\mathrm{V})/p_T(\mathrm{H})\|_{kinfit}$ | ratio between vector boson and H transverse momenta after kinematic-fit | — | — | ✓ |
| | $\sigma(\mathrm{H})\|_{kinfit}$ | H invariant mass resolution from kinematic fit | — | — | ✓ |

Merged

# ParticleNet architecture and inputs

➔ ParticleNet harness the Dynamic Graph CNN (DGCNN) [arXiv:1801.07829]

- harness EdgeConv operation to pass on learned features for each point which is interpreted as "coordinates" in high-dim latent space
- increasing layer size for EdgeConv
- fully connected layer transfer the feature space to N outputs

➔ Input feature

- up to 100 PF candidates per jet with 20 features + 2 coordinates ($\eta_{rel}$, $\phi_{rel}$)
- up to 10 SVs per jet with 11 features + 2 coordinates ($\eta_{rel}$, $\phi_{rel}$)

➔ Training performed by the framework weaver

➔ More details in [CMS-DP-2020-002]

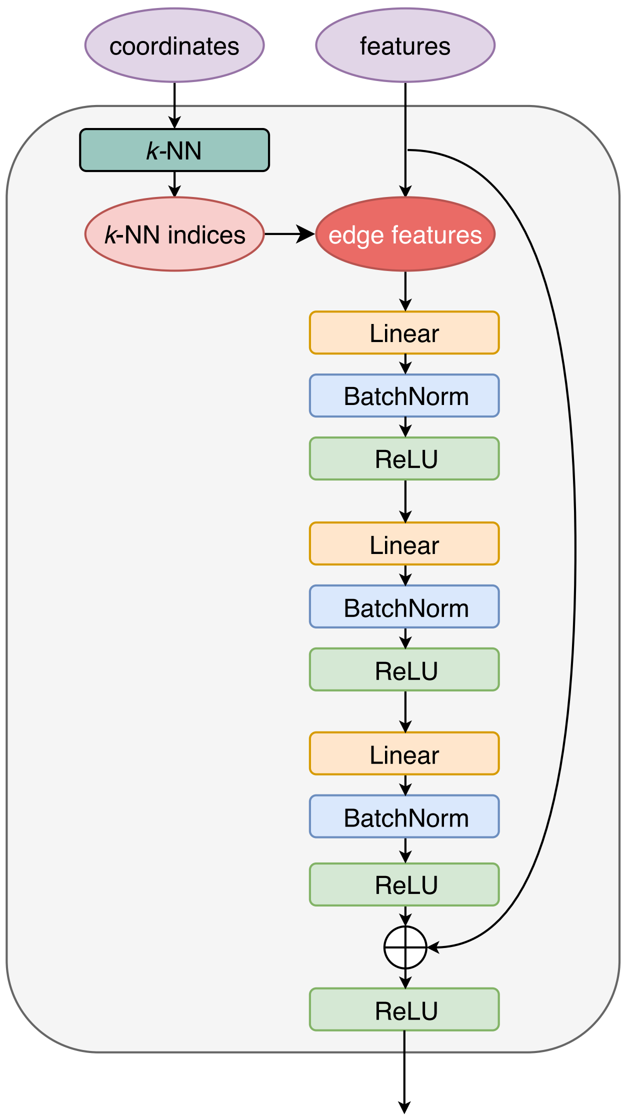


EdgeConv block

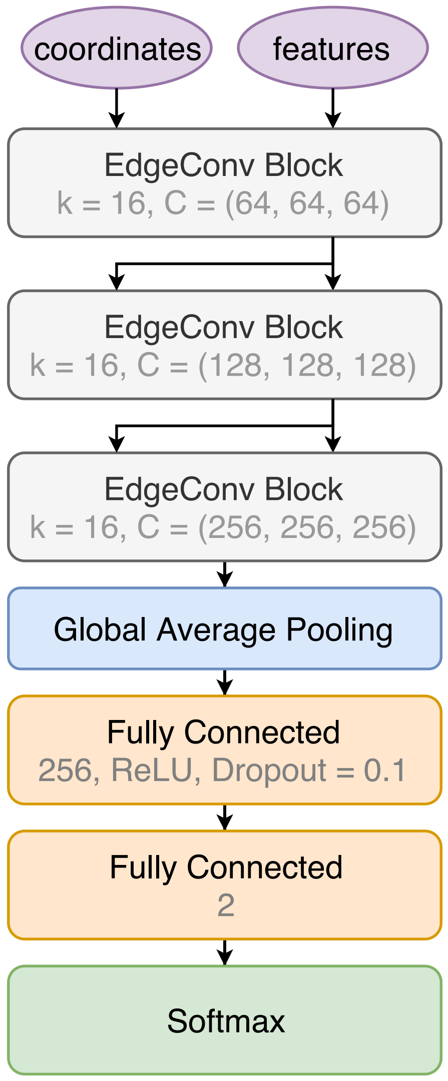


ParticleNet full architecture

Merged

# ParticleNet calibration

- ➔ ParticleNet tagger calibration for H→cc signal jet
  - ❖ use g→cc from QCD multi-jet events as a proxy to H→cc jets
  - ❖ ***sfBDT***: select a phase-space from g→cc that resembles H→cc jets
    - provide a handle to adjust the proxy–signal jet similarity
  - ❖ simultaneous fit in pass and fail tagger region
    - fit variable: $\log(m_{SV})$
    - 3 rate parameters for c(cc), b(bb), light
    - improved treatment of the systematics
  - ❖ details in [CMS-DP-2022-005]

cc-tagging scale factors

Passing category

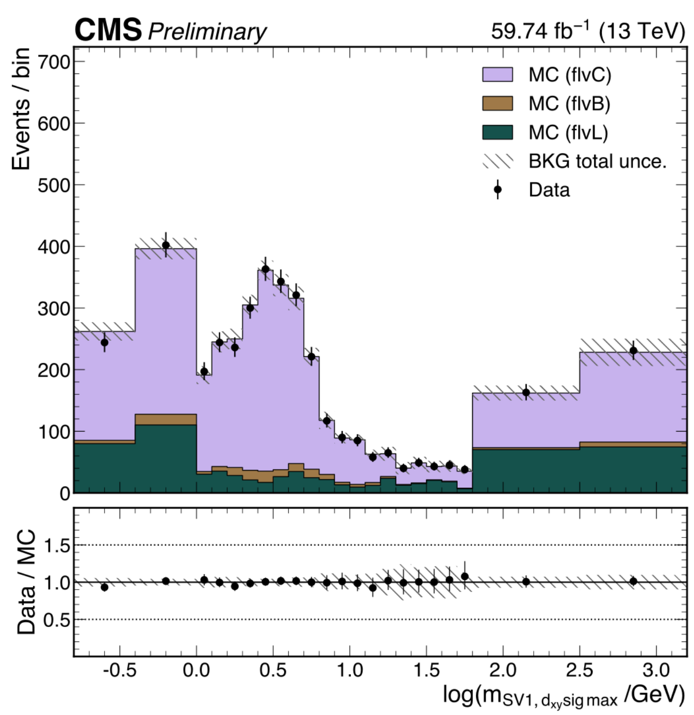


Failing category

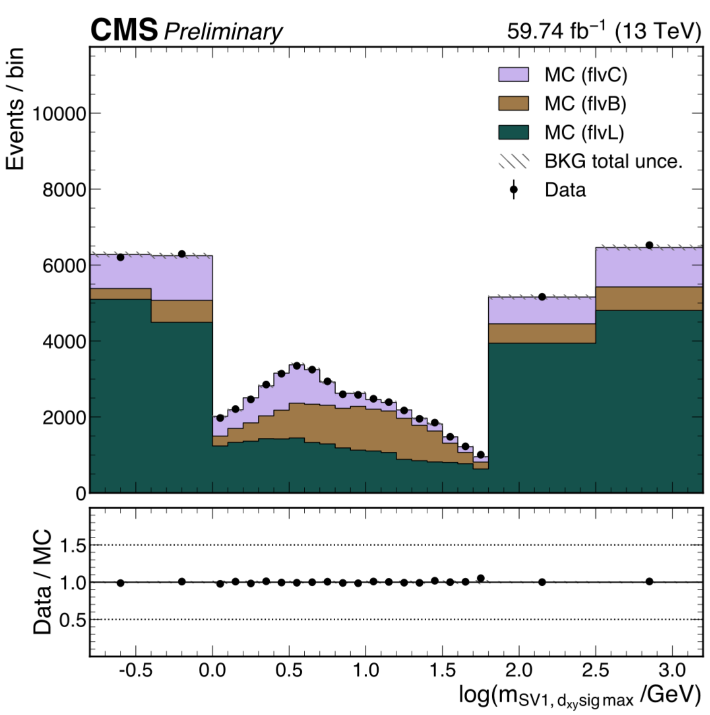


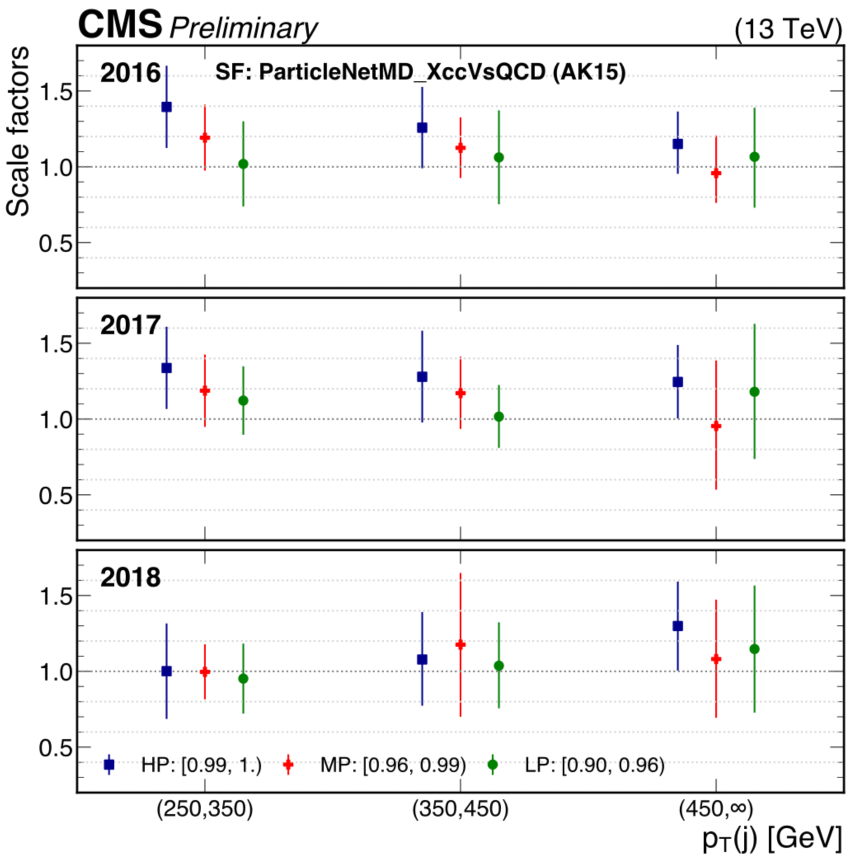

Merged

# kinematic BDT for merged-jet topology

- ➔ Kinematic BDT developed to better separate VH signals from major backgrounds (V+jets, tt̄)
  - ❖ using only event kinematics, not intrinsic property (e.g. mass/flavour) of the AK15 jets
    - ‣ BDT largely uncorrelated with $m_{reg}$ and ParticleNet cc-tagger
  - ❖ low-BDT CR defined based on kinematic BDT

*inclusive BDT distribution for 3 channels*

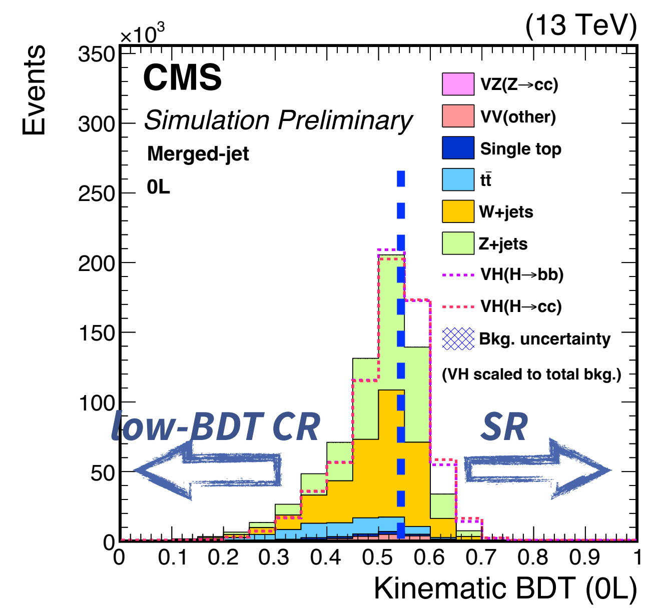


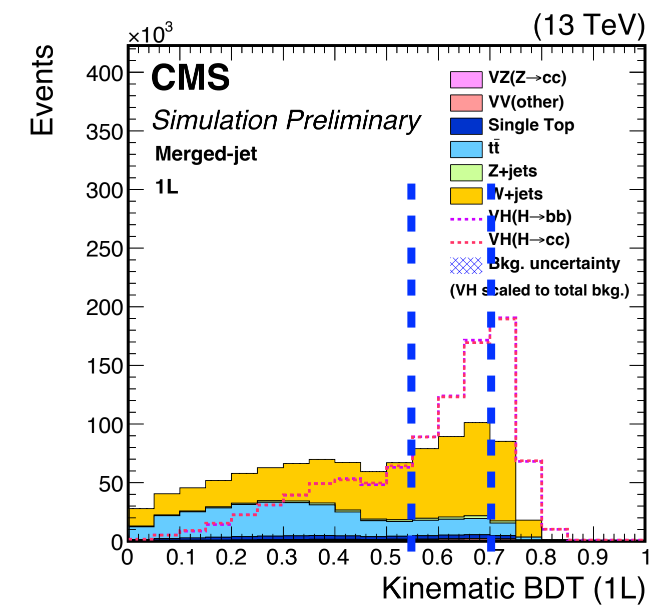


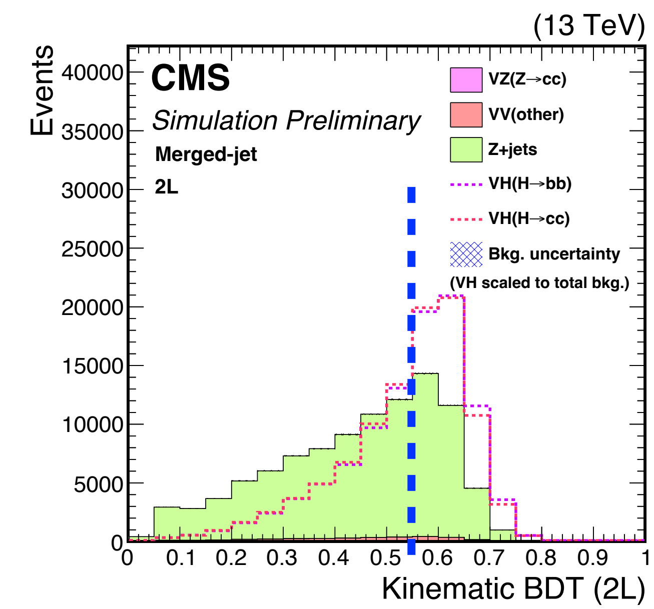


*input variables to kinematic BDT*

| Variable | Description | 0-lepton | 1-lepton | 2-lepton |
|---|---|---|---|---|
| $p_T(V)$ | vector boson transverse momentum | ✓ | ✓ | ✓ |
| $\Delta R(\ell,\ell)$ | angular separation between the two leptons | | | ✓ |
| $p_T(H_{cand})$ | $H_{cand}$ transverse momentum | ✓ | ✓ | ✓ |
| $\lvert\eta(H_{cand})\rvert$ | absolute value of the $H_{cand}$ pseudorapidity | ✓ | | |
| $\Delta\phi(V, H_{cand})$ | azimuthal angle between vector boson and $H_{cand}$ | ✓ | ✓ | ✓ |
| $p_T^{miss}$ | missing transverse momentum | | ✓ | |
| $\Delta\eta(H_{cand}, \ell)$ | difference in pseudorapidity between $H_{cand}$ and the lepton | | ✓ | |
| $\Delta\eta(H_{cand}, V)$ | difference in pseudorapidity between $H_{cand}$ and vector boson | | | ✓ |
| $\Delta\eta(H_{cand}, j)$ | min. difference in pseudorapidity between $H_{cand}$ and small-$R$ jets | ✓ | ✓ | ✓ |
| $\Delta\eta(\ell, j)$ | min. difference in pseudorapidity between the lepton and small-$R$ jets | | ✓ | |
| $\Delta\eta(V, j)$ | min. difference in pseudorapidity between vector boson and small-$R$ jets | | | ✓ |
| $\Delta\phi(\vec{p}_T^{miss}, j)$ | azimuthal angle between $\vec{p}_T^{miss}$ and closest small-$R$ jet | ✓ | | |
| $\Delta\phi(\vec{p}_T^{miss}, \ell)$ | azimuthal angle between $\vec{p}_T^{miss}$ and lepton | | ✓ | |
| $m_T$ | transverse mass of lepton $\vec{p}_T + \vec{p}_T^{miss}$ | | ✓ | |
| $N_j$ | number of small-$R$ jets | ✓ | ✓ | ✓ |

# Merged-jet: analysis strategy

➔ Signal region selections and fit

- kinematic BDT → cc-tagging discriminant (ParticleNet score) → fit on regressed Higgs candidate mass